1 **MATERNAL OBESITY CAUSES FETAL CARDIAC HYPERTROPHY AND ALTERS ADULT OFFSPRING**
2 **MYOCARDIAL METABOLISM IN MICE**

3

4 Owen R. Vaughan[1], Fredrick J. Rosario[1], Jeannie Chan[2], Laura A. Cox[2], Veronique Ferchaud-Roucher[1], Karin
5 A. Zemski-Berry[3], Jane E.B. Reusch[3], Amy C. Keller[3], Theresa L. Powell[1,4] and Thomas Jansson[1]

6 [1]Department of Obstetrics and Gynecology, University of Colorado Anschutz Medical Campus, Aurora, CO,
7 USA

8 [2]Department of Molecular Medicine, Wake Forest School of Medicine, Winston-Salem, NC, USA

9 [3]Department of Medicine, Division of Endocrinology, Metabolism and Diabetes, University of Colorado
10 Anschutz Medical Campus, Aurora, CO, USA and Rocky Mountain Regional VA Medical Center, Aurora, CO,
11 USA

12 [4]Department of Pediatrics, University of Colorado Anschutz Medical Campus, Aurora, CO, USA

13

14 **Short title:** Maternal obesity alters offspring heart metabolism

15 **Manuscript category:** Original article

16 **Correspondence:**

17 Owen R. Vaughan, PhD

18 Department of Obstetrics and Gynecology

19 University of Colorado Anschutz Medical Campus

20 12700 E19th Avenue

21 Aurora, CO, USA

22 owen.vaughan@CUAnschutz.edu

23 Phone: (303) 724-8622

24 Fax: (303) 724-3512

25

26 **Total word count:** 5416 words

27

28 **Key words:** diabetes mellitus, gestational; fetal macrosomia; peroxisome proliferator activated

29 receptor gamma; positron emission tomography; heart failure, diastolic

30   **ABSTRACT**

31   Obesity in pregnant women causes fetal cardiac dysfunction and increases offspring cardiovascular

32   disease risk but its effect on myocardial metabolism is unknown. We hypothesised that maternal obesity

33   alters fetal cardiac expression of metabolism-related genes and shifts offspring myocardial substrate

34   preference from glucose towards lipids. Female mice were fed control or obesogenic diets before and

35   during pregnancy. Fetal hearts were studied in late gestation (embryonic day, E18.5; term≈E21) and

36   offspring were studied at 3, 6, 9 or 24 months postnatally. Maternal obesity increased heart weight and

37   peroxisome proliferator activated receptor γ (*Pparg*) expression in female and male fetuses and caused

38   left ventricular diastolic dysfunction in the adult offspring. Cardiac dysfunction progressively worsened

39   with age in female, not male, offspring of obese dams, compared to age-matched controls. In 6-month-

40   old offspring, exposure to maternal obesity increased cardiac palmitoyl carnitine-supported

41   mitochondrial respiration in males and reduced myocardial ^{18}F-fluorodeoxyglucose uptake in females.

42   Cardiac *Pparg* expression remained higher in adult offspring of obese than control dams and correlated

43   with contractile and metabolic function. Maternal obesity did not affect cardiac palmitoyl carnitine

44   respiration in females or ^{18}F-fluorodeoxyglucose uptake in males, or alter cardiac ^{3}H-oleic acid uptake,

45   pyruvate respiration, lipid content or fatty acid/glucose transporter abundance in offspring of either sex.

46   The results support our hypothesis and show that maternal obesity affects offspring cardiac metabolism

47   in a sex-dependent manner. Persistent upregulation of *Pparg* expression in response to overnutrition *in*

48   *utero* may mechanistically underpin programmed cardiac impairments and contribute to cardiovascular

49   disease risk in children of women with obesity.

50 **INTRODUCTION**

51 The global prevalence of obesity in women of reproductive age is rapidly increasing [1]. Obesity in pregnant

52 women predisposes their children to metabolic syndrome and a range of non-communicable diseases

53 throughout life, thereby placing a substantial burden on the health of the population [2]. Children of women

54 who have obesity during pregnancy are at 30% greater risk for cardiovascular disease in adulthood [3]. Diet-

55 induced obesity in pregnant animals similarly leads to abnormal cardiovascular function in their adult

56 offspring, irrespective of postnatal diet [4, 5], demonstrating that lifelong phenotype is programmed before

57 birth. However, the mechanisms underlying cardiometabolic programming by maternal obesity remain

58 poorly understood and neither the specific programming signals nor their primary targets in the fetus

59 have been clearly identified.

60 Fetuses of obese women have cardiac hypertrophy and contractile dysfunction as early as the first

61 trimester [6, 7], and these abnormalities persist at least into childhood [8]. Similarly, in experimental animals,

62 maternal obesity increases fetal heart size, wall thickness, cardiomyocyte size, inflammation and collagen

63 content, and impairs contractility [9-12]. These data suggest that maternal obesity directly affects the heart

64 *in utero*.

65 Maternal obesity alters placental transport and fetal delivery of glucose and lipids, in both humans and

66 experimental animals [13-16]. Maternal obesity also increases fetal cardiac lipid storage in sheep [11], and

67 impairs glucose uptake and mitochondrial respiration in isolated cardiomyocytes from the offspring in

68 rodents [17, 18]. Impaired diastolic function in people with diabetes is associated with increased cardiac fatty

69 acid uptake and oxidation, but reduced glucose uptake [19, 20] whilst genetic modifications that increase

70 cardiac lipid uptake in mice cause contractile dysfunction [21]. Whether abnormal cardiac glucose and lipid

71 metabolism contributes to cardiac dysfunction in the offspring of pregnancies complicated by maternal

72 obesity remains unknown.

73   We have developed a mouse model of maternal obesity associated with fetal overgrowth that closely

74   replicates the phenotype of obese pregnant women in terms of maternal physiology, placental nutrient

75   transport and fetal growth [13]. In this model, administration of adiponectin to increase maternal

76   concentrations of this metabolic hormone in obese dams, to the levels observed in control animals,

77   normalises placental nutrient transport, prevents fetal overgrowth and mitigates cardiac diastolic

78   dysfunction in the adult offspring [22, 23]. In the current study, we used our established model to determine

79   the effect of maternal obesity on the fetal cardiac transcriptome and on cardiac contractile and metabolic

80   function in the adult offspring. We hypothesised that maternal obesity alters fetal cardiac expression of

81   metabolism-regulating genes and increases lipid metabolism but reduces glucose metabolism in hearts of

82   adult offspring. We also measured cardiac histone acetylation, which is linked to heart failure [24] and is

83   sensitive to nutrient availability [25], to determine whether it plays a role in fetal cardiac programming by

84   maternal obesity.

85 **MATERIALS AND METHODS**

86 **Animals**

87 All procedures were conducted with approval from the Institutional Animal Care and Use Committee of

88 the University of Colorado. Female C57BL6/J mice, proven breeders, were fed *ad libitum* with an

89 obesogenic diet (Ob, n=31) consisting of high fat pellets (Western Diet D12079B, 41 kcal% fat)

90 supplemented with sucrose solution (20 %), or a control diet (Con, D12489B, 10.6 kcal% fat, n=50). All

91 animals had *ad libitum* access to fresh water and were housed under standard 12hr: 12hr dark:light

92 conditions. When females fed the Ob diet had gained 25% of their initial body weight, they were mated

93 overnight with stud males. Age-matched Con females were mated simultaneously. Successful mating was

94 confirmed by the presence of a copulatory plug the following morning, designated embryonic day (E) 0.5

95 (term ~E19.5). Pregnant females were subsequently housed in pairs. On E18.5, a subset of Con (n=5) and

96 Ob (n=5) dams were euthanised by CO_2 asphyxiation and cervical dislocation. The uterus was exposed,

97 fetuses were excised and weighed then their hearts were dissected, weighed and snap frozen in liquid N_2.

98 A fetal tail snip was also collected for subsequent determination of sex, by *Zfy-1* genotyping [26]. The

99 remaining Con and Ob dams delivered naturally at term and continued to consume their respective diets

100 throughout lactation, until all pups were weaned onto standard chow at age 4 weeks. Pups were

101 subsequently housed in same sex groups, from multiple litters. In total, 187 offspring were used in the

102 study.

103 **Experimental procedures**

104 **Echocardiography.** Cardiac structure and function were assessed using transthoracic echocardiography in

105 a subset of offspring at both 3 and 6 months of age (females n=10 Con, 6 Ob; males n= 7 Con, 7 Ob), as

106 described in Supplemental Methods. One week after the second echocardiography assessment, offspring

107 were fasted for 4 hr then euthanised by CO_2 asphyxiation and cervical dislocation. Hearts were perfused

108   with PBS then excised and weighed. The left ventricle was dissected and snap frozen in liquid N_2 for gene

109   expression analyses. Thirty-nine additional animals that had not undergone echocardiography were also

110   euthanised at age 6 months, and tissues collected in the same manner for gene expression and lipidomic

111   analyses.

112   Separate cohorts of offspring underwent echocardiographic assessment by the same operator at ages 9

113   months (n=28) or 24 months (n=22), without being imaged at earlier time points. These animals were

114   euthanised seven days after echocardiography and their tissues collected for use in other studies.

115   **Positron emission tomography.** Cardiac glucose uptake was assessed *in vivo* in forty-eight 6-month old

116   offspring using positron emission tomography (PET) with ^{18}F-fluorodeoxyglucose (^{18}F-FDG) tracer. Animals

117   were fasted for 4 hours prior to the study then anaesthetised (2% isoflurane, inhaled) and positioned in

118   dorsal recumbency on a warming pad at 37°C. Animals were then placed inside a PET imaging system

119   (Inveon microPET, Siemens Medical, Knoxville, TN, USA) and a bolus dose of ^{18}F-FDG was administered

120   intravenously, to the tail vein (250uCi). Fifteen dynamic PET image frames were collected at successive

121   timepoints over a period of 35 minutes. A whole-body computerised tomography image, without contrast

122   agent, was subsequently collected to confirm anatomical distribution of the ^{18}F-FDG tracer. Mice were

123   removed from the scanner, recovered from anaesthesia and housed in a lead-shielded cage with *ad*

124   *libitum* access to food and water, before being returned to their home cage 24 hr later.

125   Ten animals that underwent PET imaging were excluded from the subsequent analysis because (a) they

126   did not tolerate anaesthesia, (b) poor tail vein patency hindered tracer infusion, or (c) movement

127   interfered with collection of dynamic frame images. Dynamic frame PET images were assembled for each

128   animal and voxel intensities (radioactivity) determined for manually defined regions of interest in the left

129   ventricular myocardium (study compartment) and lumen (reference compartment). Radioactivity at each

130   timepoint, within each compartment, was corrected for decay, animal weight and the amount of tracer

131 injected. The ratio of radioactivity in the left ventricular myocardium to that in the reference compartment

132 was then plotted against normalised time from tracer injection, according to the Patlak method [27].

133 Separate linear regression lines were fitted to data from Con and Ob groups and the slopes compared by

134 extra sum-of-squares F test, within each sex. The slope of the Patlak plot represents the clearance of [18]F-

135 FDG from the blood, into the myocardium.

136 This group of animals was euthanised seven days after imaging, as described above. A portion of the left

137 ventricle was placed into ice-cold biopsy preservation solution (BIOPS [28]) for analysis of mitochondrial

138 respiration within ~3 hours.

139 **_In vivo_ left ventricular ^{3}H-oleic acid uptake.** Cardiac fatty acid uptake was quantified in 20 six-month old

140 offspring using a radioactive tracer, as described previously [29]. Briefly, 4.5µCi ^{3}H-oleic acid (NET289001MC,

141 Perkin Elmer), was dried down under N_2 then resuspended in PBS and combined 1:1 with 40% fatty-acid

142 free bovine serum albumin to a final volume of 200µl, at 37°C with shaking. Mice were anaesthetised

143 with ketamine and xylazine (_i.p._), the tail vein canulated and the BSA-complexed ^{3}H-oleic acid tracer

144 delivered as a bolus. Up to five minutes later, mice were euthanised with sodium pentobarbital solution

145 (_i.v._), rapidly exsanguinated and the heart perfused with PBS. Plasma was separated from blood by

146 centrifugation. Left ventricles (LV) were dissected, weighed then digested for 48 hr at 50°C in Biosol

147 (National Diagnostics). LV and plasma radioactivity were determined by liquid scintillation counting and

148 ^{3}H-oleic acid clearance calculated from the ratio of total LV counts to the area under the curve of plasma

149 counts versus time from tracer infusion, divided by LV weight.

150 **Biochemical and molecular analyses**

151 **RNA extraction, sequencing and Ingenuity Pathway Analysis.** Heart tissues were collected from male and

152 female fetuses within litters from Con (n=5) and Ob (n=5) dams and stored at -80°C. Individual frozen

153 tissue samples (~10 mg) were homogenized in TRI Reagent and total RNA was isolated using Direct-zol

154   RNA MiniPrep kits (Zymo Research, Irvine, CA) according to the manufacturer's instructions. After eluting

155   RNA from the Zymo-Spin column in 50 µl DNase/RNase-free water, RNA quality was assessed using an

156   Agilent 2100 Bioanalyzer (Agilent Technologies, Inc., Santa Clara, CA). RNA concentration was quantified

157   using Qubit RNA HS assay kits and a Qubit 2.0 Fluorometer (Thermo Fisher Scientific, Wilmington, DE).

158   Total RNA was stored at -80°C. Differentially expressed genes between Con and Ob fetuses were identified

159   and functionally annotated, as described in the Supplementary Methods.

160   **High resolution *in situ* respirometry.** Carbohydrate- and lipid supported rates of mitochondrial respiration

161   were assessed in cardiac muscle from 6-month old offspring, using high resolution respirometry. Biopsies

162   of fresh left ventricular tissue in ice-cold BIOPS solution were dissected under magnification into myofiber

163   bundles of approximately 1 mg. The sarcolemmal membrane was permeabilized by incubating in saponin

164   solution ($40\mu g \ ml^{-1}$, 20 min) then washed, accurately weighed and placed in an oxygraph chamber

165   (Oroboros O2k Respirometer), in respiration medium (MIRO5, [28]) with blebbistatin (5mM) to inhibit

166   muscle contraction. Medium was equilibrated with O_2 gas to an initial dissolved concentration of 400µM

167   and the chamber was sealed. Catalase was also added to the respiration medium to allow liberation of

168   oxygen by H_2O_2 addition during the experiment, thus retaining dissolved O_2 concentration between 300

169   µM and 400 µM.

170   O_2 consumption rate was determined during the sequential addition of one of two different combinations

171   of substrates and inhibitors, designed to determine the basal and maximal rates of carbohydrate- and

172   lipid-supported respiration, respectively. In the first assay, pyruvate (5mM) and malate (2mM) were

173   added to the oxygraph chamber to supply the electron transport chain via reduced intermediates

174   generated in the citric acid cycle. In the second assay, palmitoyl carnitine (5µM) and malate (1mM)

175   supplied electrons via mitochondrial β-oxidation. In both cases, leak state oxygen consumption was first

176   measured in the absence of ADP. Then ADP (2mM) was introduced to measure basal respiration rate,

177   coupled to ATP synthase activity. Glutamate (3mM) and succinate (6mM) were subsequently provided to

178   support direct electron flux to complex I and II of the electron transport chain, allowing maximum

179   oxidative phosphorylation capacity to be measured. ATP synthase activity was abolished using oligomycin

180   (4µg/ml), to measure leak state oxygen consumption supported by both fatty acid oxidation and direct

181   complex I/II electron entry. Finally, FCCP (carbonyl cyanide 4-(trifluoromethoxy)phenylhydrazone) was

182   added in increments of 0.5µM to permeabilise the inner mitochondrial membrane, until maximal,

183   uncoupled oxygen consumption was achieved, measuring electron transport chain capacity. Respiration

184   rates were corrected to fresh tissue mass. Coupling efficiencies for each of the two combinations of

185   substrates was calculated as 1 minus the ratio (leak state respiration/maximal electron transport chain

186   capacity).

187   **Targeted lipidomic analyses.** Cardiac triglyceride contents were determined by colorimetric assay

188   (MAK266, Sigma-Aldrich). Myocardial content of individual fatty acids, ceramides and diacylglycerol

189   species was measured in adult offspring using targeted mass spectrometry, described in Supplementary

190   Methods.

191   **Western blot.** Fatty acid and glucose transporter protein abundance was measured in cardiac tissue from

192   6-month old offspring using western blotting. Frozen heart samples were homogenised in hepes-tris

193   buffered saline with protease and phosphatase inhibitors (Sigma Aldrich). Samples were then loaded in

194   Laemmli buffer, resolved by polyacrylamide gel electrophoresis and transferred to polyvinylidene fluoride

195   membrane. Membranes were incubated with primary antibodies to CD36, FATP1, FATP6, GLUT1 and

196   GLUT4 then with a horseradish peroxidase linked secondary antibody and visualised using enhanced

197   chemiluminescence reaction and a gel imaging system. Protein abundance was determined by

198   densitometry of specific bands, corrected for protein loading (amido black stain).

199   **Gene expression.** Cardiac expression of selected mRNAs related to lipid metabolism was determined in a

200   targeted manner using qRT-PCR. RNA was extracted from frozen ventricular tissue from 6-month-old Con

201   (females n=9, males n=11) and Ob (females n=10, males n=10) offspring using a commercially available kit

202   (RNeasy Plus mini Kit, Qiagen) then reverse transcribed to cDNA (High Capacity cDNA Reverse

203   Transcription kit, Applied Biosystems). Relative expression of target mRNAs was determined by qRT-PCR

204   using SYBR Green chemistry and forward and reverse primers, as detailed in Supplemental Table 1. The

205   efficiency of all primer pairs was confirmed to be between 80 and 110% by calculating the linear gradient

206   of the relationship between average Ct value and dilution factor for a 5-fold serially diluted standard curve

207   of pooled cDNA. PCR product size was validated by agarose gel electrophoresis. Gene expression was

208   determined relative to the geometric mean of *Rna18s* and *Rps29* expression using the ddCt method.

209   **Statistics.** Results are presented as mean ± SEM. All statistical analyses were conducted separately in

210   female and male offspring. Normality of data was assessed by Shapiro-Wilk test. Echocardiographic

211   measurements of cardiac function and morphometry were analysed by two-way ANOVA, with maternal

212   obesity and postnatal age as independent factors. When there was a significant interaction between these

213   two factors, the simple effect of maternal obesity at each age was assessed by Sidak post-hoc test. For all

214   other measurements, Con and Ob groups were compared by Student's t-test or by Mann-Whitney test, if

215   data did not conform to a normal distribution. Analyses of lipidomic data were corrected for multiple

216   comparisons using the Holm-Sidak method. Linear relationships between variables were determined by

217   Pearson's correlation. In all cases, significance was taken at the level P<0.05.

218

219 **RESULTS**

220 **Maternal obesity in pregnant mice induces fetal cardiac hypertrophy and transcriptional activation of**

221 **lipid metabolism genes**

222 Maternal obesity increased fetal heart weight at E18.5, as a percentage of total body weight, in both male

223 and female fetuses (Fig. 1A, B). Absolute heart and body weights were also greater in fetuses of obese

224 dams, compared to controls (Table 1).

225 Maternal obesity concomitantly altered the expression of 841 genes in the hearts of female fetuses and

226 764 genes in the hearts of male fetuses, with 66 genes commonly altered in both sexes (Suppl. Fig. 1A, B).

227 Ingenuity analysis predicted inhibition of processes related to neoplasia and DNA repair/synthesis in male

228 fetal hearts, and pathways related to function, quantity and movement of immune cells in female fetal

229 hearts, in obese compared to control dams (z-score <-1.7, top ten functions by P-value, Fig. 1C, D). By

230 contrast, maternal obesity activated synthesis of lipid and metabolism of membrane lipid derivatives in

231 male fetuses, and uptake of monosaccharides and carbohydrates in female fetuses (activation z-score >

232 1.7, top-ten functions by P-value, Fig. 1 E, F). Transport of molecules was consistently activated by

233 maternal obesity in both males and females (Fig. 1G).

234 The activated downstream functions related to molecular transport, carbohydrate and lipid metabolism

235 encompassed an overlapping suite of differentially expressed genes, several of which were commonly

236 regulated by maternal obesity in male and female fetuses (Fig. 1H). Specifically, maternal obesity

237 upregulated *Pparg*, the nuclear peroxisome proliferator activated receptor implicated in lipogenesis,

238 *Cd36,* a plasma membrane fatty acid translocase, and *Prkaa1*, the catalytic subunit of cytoplasmic AMP-

239 activated protein kinase (AMPKa1), in fetuses of both sexes (Fig. 1H-J). Network analysis of direct

240 molecular interactions between the differentially expressed, metabolism-related genes indicated that

241 *Pparg* was a critical node in both the female and male fetal transcriptomic response (Suppl. Fig. 1C, D).

242   Furthermore, when unsupervised regulator effects analysis was used to link the annotated downstream

243   functions of differentially expressed genes to upstream effectors, a network of genes activated by

244   *Ppargc1a* and including *Cd36* and the triglyceride synthesis enzyme, *Lpin1*, was predicted to promote lipid

245   synthesis in male fetal hearts in response to maternal obesity (Suppl. Fig 1E.). Taken together, the

246   transcriptomic data were most consistent with maternal obesity promoting cardiac lipid metabolism in

247   male and female fetuses, by increasing expression of genes related to fatty acid uptake, lipid synthesis

248   and oxidation.

249   **Maternal obesity in pregnant mice causes age- and sex-dependent diastolic dysfunction and left**

250   **ventricular dilation in adult offspring.**

251   In male offspring, E/A and E'/A' ratios of left ventricular diastolic function declined overall with increasing

252   postnatal age from 3 to 24 months and were further impaired by maternal obesity at all time points (Fig.

253   2A, C). Maternal obesity also reduced E/E' ratio in males, with significant differences apparent between

254   Con and Ob groups in both the youngest and oldest offspring studied (Fig. 2E). By contrast, the effect of

255   maternal obesity on diastolic function in female offspring depended on the age at which they were

256   studied. Three months after birth, neither E/A nor E'/A' ratio differed between Con and Ob female

257   offspring (Fig 2B, D). Six months after birth, E'/A' ratio, but not E/A ratio, was reduced, and by 9 months

258   both E'/A' and E/A ratios were lower in Ob compared to Con females. Finally, at age 24 months, E/A ratio

259   was higher in Ob than Con female offspring, whereas E'/A' ratio was similar in the two groups, indicating

260   a more severe state of diastolic dysfunction with pseudonormal filling pattern. E/E' ratio was lower in Ob

261   than Con female offspring, irrespective of age (Fig. 2F). Therefore, maternal obesity caused diastolic

262   dysfunction in adult offspring of both sexes, albeit the effect was later in onset but faster in progression

263   in females than males.

264 In males, maternal obesity increased end-diastolic volume in 2-year-old offspring and increased end-

265 systolic volume irrespective of age (Fig. 3A, C). By contrast, in female offspring, maternal obesity increased

266 left ventricular end-diastolic volume, but not end-systolic volume (Fig. 3B, D). Both left ventricular wall

267 thickness and systolic function, measured by ejection fraction and fractional shortening, increased

268 modestly with age in male and female mice but were not affected by maternal obesity (Suppl. Fig 2). When

269 tissues were weighed at necropsy in 6-month old offspring, heart weight was significantly greater in Ob

270 than Con females as an unadjusted value, but not expressed as a percentage of body weight (Table 2).

271 However, none of the other measurements of body, heart or ventricle weight differed between Con and

272 Ob offspring at this age.

273 **Maternal obesity alters cardiac metabolism in adult offspring in a sex-specific manner**

274 ***Gene expression***. Maternal obesity upregulated *Pparg* expression in both male and female 6-month old

275 offspring of obese dams, compared to controls (Fig. 4A, B). *Cd36* and *Prkaa1* expression were also higher

276 in Ob than Con male offspring hearts, but not in females (Fig. 4). In male offspring, maternal obesity

277 increased expression of downstream *Pparg* targets related to lipid synthesis and storage (*Fasn, Plin2,*

278 *Srebp1)* and lipid oxidation (*Pgc1a, Cpt1b, Acox1*) but did not alter *Pgc1b, Cpt1a, Mcad, Hoad, Pdk4* or

279 *Ucp3* expression (Fig. 4A). In female offspring, maternal obesity upregulated *Fasn* but did not affect

280 expression of any of the other downstream mediators of lipid metabolism studied (Fig. 4B). When adult

281 male offspring from control and obese dams were combined, there was a strong inverse correlation

282 between cardiac *Pparg* gene expression and E/E' ratio (Fig. 4C). In female offspring, there was a strong

283 correlation between cardiac *Pparg* expression and left-ventricular end-diastolic volume (Fig. 4D). *Cd36*

284 expression in female offspring also positively correlated with E/A ratio and inversely correlated with wall

285 thickness at diastole, whilst both *Pdk4* and *Hoad* expression correlated with wall thickness at systole and

286 end-diastolic volume (Suppl. Table 2). There were no other significant correlations between cardiac gene

287 expression and the measured echocardiographic and morphometric outcomes in adult offspring (Suppl.

288   Table 2). Therefore, transcriptional upregulation of *Pparg* expression and lipid metabolism persisted in

289   the offspring of obese dams and was linked to cardiac functional and structural phenotype in male and

290   female offspring.

291   ***Lipid metabolism.*** Left ventricular ^{3}H-oleic acid clearance *in vivo* was greater in female than male offspring

292   of control dams (Suppl. Fig. 3A). However, cardiac fatty acid clearance did not differ significantly between

293   Ob offspring and their Con counterparts of the same sex (Fig. 5A, B). Maternal obesity reduced FATP6

294   transporter protein abundance in hearts of female, but not male offspring, and did not affect CD36 or

295   FATP1 protein abundance (Table 3).

296   In male offspring, maternal obesity increased cardiac palmitoyl carnitine respiration in the leak state

297   (+oligomycin), when palmitoyl carnitine was supplied in combination with malate, glutamate and

298   succinate (Fig. 5C). Maximal oxidative phosphorylation-coupled palmitoyl carnitine respiration and

299   electron transport chain capacity (+FCCP) also tended to be higher in Ob than Con male offspring hearts

300   (Fig. 5C). However, maternal obesity had no effect on either coupled or leak respiration supported by

301   palmitoyl carnitine alone in male offspring (Fig. 5C), or on any of the rates of fatty acid supported

302   respiration in female offspring hearts (Fig. 5D). The coupling efficiency of fatty acid supported respiration

303   correlated with cardiac *Pparg* expression in male offspring (Fig. 5E). However, there were no overall

304   differences in coupling efficiency between Con and Ob offspring (Suppl. Table 3).

305   Maternal obesity did not alter adult offspring cardiac fatty acid content (Suppl. Table 4) or triglyceride

306   content (females Con 7.7 ± 2.2 µg/mg, Ob 9.3 ± 2.2 µg/mg; males Con 22.9 ± 5.0 µg/mg, Ob 32.7 ± 6.2

307   µg/mg). Maternal obesity reduced offspring cardiac 1,2-18:2/18:1 DAG content but did not alter

308   abundance of the other DAGs measured in adult male offspring and had no effect on any of the DAGs in

309   female offspring hearts (Suppl. Table 5). There was no difference in ceramide content between Con and

310   Ob offspring (Suppl. Table 6).

311 ***Carbohydrate metabolism.*** Myocardial glucose uptake, determined using PET as the rate of clearance of

312 ^{18}F-deoxyglucose from plasma into the left ventricle, was greater in male than female control offspring

313 (Suppl. Fig. 3B, C). Maternal obesity reduced myocardial glucose uptake in female but not male offspring

314 (Fig. 6A-D) but did not alter cardiac GLUT1 or GLUT4 abundance in offspring of either sex (Table 3). There

315 were no differences between Con and Ob offspring in the rates of pyruvate-supported mitochondrial

316 respiration in cardiac muscle *ex vivo* (Fig. 6E, F). Similarly, neither histone H3 protein abundance nor

317 acetylation differed between Con and Ob offspring (Fig. 7).

318

319

320 **DISCUSSION**

321 This is the first study in mice to link the effects of maternal obesity on fetal cardiac morphology and gene

322 expression with alterations in cardiac contractile and metabolic function in the adult offspring. The results

323 show that maternal obesity causes fetal cardiac hypertrophy *in utero*, in association with transcriptomic

324 changes consistent with altered cardiac carbohydrate and lipid metabolism. We also report that maternal

325 obesity impairs cardiac diastolic function in both male and female adult offspring, up to 2 years after birth,

326 but the progression of cardiac dysfunction with age is sex dependent. The impairments in contractile

327 function were accompanied by persistent *Pparg* upregulation and altered carbohydrate and lipid

328 metabolism in female and male offspring, respectively. The study therefore indicates that cardiac

329 metabolism is programmed by *in utero* exposure to maternal obesity and contributes to cardiac

330 dysfunction in later life.

331 The hypertrophic effects of maternal obesity on fetal heart and left ventricle weight were similar in female

332 and male fetuses and consistent with that reported previously in other experimental animals [9-12] and

333 pregnant women [6, 7]. In contrast, the effect on the fetal cardiac transcriptome strongly depended on fetal

334 sex, with less than 10% of the differentially expressed genes shared between females and males. Based

335 on bioinformatic analysis of the differentially expressed genes, the gross hypertrophic effect did not

336 appear to be explained by cellular processes that were transcriptionally inhibited in response to maternal

337 obesity, which were broadly related to inflammation in female fetuses and cell proliferation in male

338 fetuses. These changes could be linked to myocardial fibrotic remodelling [10, 11] or impaired cardiomyocyte

339 endowment, depending on fetal sex. However, the processes that were transcriptionally activated

340 seemed more likely to contribute to cardiac hypertrophy, because they were associated with transport,

341 uptake, synthesis and metabolism of macronutrient molecules required for cell growth and contractile

342 function. Certainly, cardiac lipid and glucose metabolism are strongly linked to cardiac dysfunction in

343 obese and diabetic adults [19, 20].

344   Our bioinformatic analysis pointed to *Pparg* as a central node in the network of differentially expressed

345   genes related to metabolism. Cardiac *Pparg* was upregulated in both female and male fetuses of obese

346   dams, consistent with previous reports in liver and skeletal muscle from fetuses of pregnant macaques

347   fed a high fat diet [30, 31]. The PPARγ protein is a transcription factor that is activated by binding with fatty

348   acid ligands and drives the expression of genes mediating fatty acid uptake and oxidation, including fatty

349   acid translocase *Cd36*, which was also upregulated in fetuses of obese dams. *Pparg* mRNA expression is

350   upregulated in adult mice fed a high fat diet [32] and cardiomyocyte-specific overexpression of *Pparg* causes

351   cardiac hypertrophy in transgenic adult mice, in association with systolic dysfunction, abnormal

352   mitochondrial architecture, increased triglyceride uptake and lipid storage and increased expression of

353   genes encoding for proteins involved in β-oxidation [21]. Our previous study showed that maternal obesity

354   increases placental lipid transport and fetal lipid load in mice [33]. Therefore, fetal cardiac hypertrophy in

355   pregnancies complicated by maternal obesity may be promoted by increased circulating fatty acid

356   availability activating PPARγ signalling in the heart.

357   The finding that maternal obesity impairs diastolic function in adult offspring up to 2 years old extends

358   our previous observations in this model [23]. These data confirm that transient cardiac hypertrophy due to

359   excess nutrition in early life leads to lasting impairments in contractile function of the heart, in common

360   with other studies in mice and their isolated cardiomyocytes [5, 18]. Since systolic function was not affected

361   by maternal obesity, the echocardiographic observations in offspring of obese dams were most consistent

362   with the phenotype of heart failure with preserved ejection fraction, which is a significant cause of

363   cardiovascular mortality in people [34]. Mild diastolic dysfunction is often subclinical and not diagnosed as

364   heart failure, but still associated with increased mortality. Our data therefore suggest diastolic dysfunction

365   or heart failure could be a contributing factor to increased later life cardiovascular morbidity in people

366   whose mothers had obesity during pregnancy [3]. To our knowledge, there have been no studies of adult

367   cardiac function in this population.

368   In contrast with the changes in fetal heart weight, the effect of maternal obesity on offspring cardiac

369   function depended on postnatal age and sex, with diastolic function consistently impaired in males but

370   progressively worsening with age in females. This may be partly explained by circulating oestrogens

371   having a cardioprotective effect in young female offspring [35]. The appearance of overt diastolic

372   dysfunction in 9-month old offspring of obese dams, with both E'/A' and E/A ratios reduced,

373   approximately coincided with declining oestradiol levels in this strain and may therefore reflect

374   diminishment of the protective oestrogen effect [36]. Unfortunately, we did not consider the influence of

375   reproductive cycles in the timing of our analyses and blood collections, preventing us from further

376   investigating the contribution of oestradiol levels. Female offspring of obese dams had most severe

377   diastolic dysfunction at 2 years of age, which is certainly after full reproductive senescence occurs

378   between 13 and 16 months [37]. Sex differences in the long-term effect of maternal obesity on the offspring

379   heart could therefore be due to sexually dimorphic changes in normal physiology and endocrinology with

380   age. This is consistent with clinical observations showing that elderly women have a higher risk of cardiac

381   dysfunction than men and are more likely to develop dysfunction in association with type 2 diabetes and

382   ventricular hypertrophy [38].

383   Our study suggests that the sex-specific effects of maternal obesity may also be linked to differences in

384   the metabolism of the heart. The results provide the first demonstration that *in vivo* cardiac metabolism

385   depends on sex in adult mice, with greater cardiac fatty acid uptake in females but greater glucose uptake

386   in males, in line with the known differences between women and men [39, 40]. Reduced *in vivo* cardiac

387   glucose uptake in adult female offspring of obese dams is consistent with the reported reduction in *in*

388   *vitro* cardiomyocyte glucose uptake when the offspring of obese mice are fed a high fat diet [18]. It also

389   reflects the pathophysiological changes in the hearts of people with type 2 diabetes [19]. Since there was no

390   accompanying change in cardiac mitochondrial capacity for carbohydrate respiration or myocardial

391   glucose transporter abundance, reduced cardiac glucose uptake may be explained by myocardial insulin

392 resistance in female offspring of obese dams. Maternal obesity has been shown to cause peripheral insulin

393 resistance, reduced cardiac insulin receptor abundance and sex-specific alterations in signalling pathways

394 downstream of the insulin receptor in the offspring heart [4, 23]. In turn, impaired glucose uptake may have

395 limited cardiac flexibility to generate ATP under conditions of high workload or low oxygen, causing

396 contractile dysfunction. Certainly, glucose uptake is positively correlated with systolic function in humans

397 [41].

398 Alterations in net cardiac lipid uptake did not explain diastolic dysfunction in the offspring of obese dams,

399 even though myocardial fatty acid uptake has been reported to increase in association with diastolic

400 dysfunction in people with diabetes [19]. Cardiac dysfunction in adult male offspring in our study may

401 instead have been related to the increase in mitochondrial fatty acid oxidation, which similarly occurs in

402 association with reduced energetic efficiency in the hearts of adult rats fed a high fat diet [42]. This effect

403 may partly be mediated by increased expression of PPARγ co-activator 1α (*Pgc1a*), which stimulates

404 mitochondrial biogenesis, and the carnitine acetyltransferase *Cpt1b*, responsible for trafficking long chain

405 fatty acids into the mitochondria. Although our observations indicated that maternal obesity most

406 robustly increased oligomycin-uncoupled β-oxidation, there was no accompanying increase in *Ucp3*

407 expression or coupling control ratio, suggesting that the effect of maternal obesity was primarily due to

408 increased activity of the β-oxidation pathway itself. Increased lipid oxidation in offspring of obese dams

409 may have caused cardiomyocyte damage by increasing production of reactive oxygen species [17]. Despite

410 increased *Plin2* and *Srebp1* expression in males, we did not find evidence of increased cardiac lipid storage

411 or altered abundance of DAG and ceramide derivatives, arguing against a role for cardiac lipotoxicity *per*

412 *se* in the offspring of obese dams. This finding contrasted with previous studies in sheep fetuses and

413 neonatal rats showing that maternal obesity increases cardiac lipid accumulation in the perinatal period

414 [9, 17]. Increased lipid oxidation may therefore outweigh increased storage in the long term. Indeed, cardiac

415 triglyceride content is reduced in adult offspring of pigs fed a high fat diet [43]. The results are therefore

416   most consistent with increased lipid oxidation underpinning cardiac dysfunction in male offspring of obese

417   dams.

418   At a molecular level, increased cardiac lipid oxidation was consistent with the persistant upregulation of

419   *Pparg* expression, compared to controls. We therefore speculate that *Pparg* upregulation causes the

420   myocardial metabolic alterations and, in turn, diastolic dysfunction in the adult male offspring. This

421   proposal is supported by the strong correlation of *Pparg* expression with E/E' ratio and respiratory

422   coupling control ratio in adult male offspring. *Pparg* expression is strongly linked to increased locus

423   specific H3K9 and H3K27 acetylation during adipogenesis [44] and maternal high fat feeding increases fetal

424   hepatic *Pparg* expression in association with increased histone acetylation [45] but we did not find any

425   changes in total cardiac H3K9 and H3K27 acetylation in this study. Therefore, the epigenetic mechanism

426   underpinning persisting upregulation of *Pparg* in the offspring of obese dams remains unclear.

427   Taken together, the results support our hypothesis that maternal obesity alters cardiac metabolism in

428   fetuses and adult offspring of obese pregnant mice. They show that the long-term effects are sex-specific

429   but associated with cardiac *Pparg* upregulation and a shift from glucose to lipid metabolism in both male

430   and female offspring of obese dams. Reduced cardiac metabolic flexibility, established *in utero*, may

431   therefore contribute to later-life cardiometabolic disease risk in children of women with obesity. The

432   findings imply that therapeutic strategies that modify the supply of nutrients to fetuses of obese women

433   may improve their later health.

434

442   **CONFLICT OF INTEREST**

443   Conflict of Interest: none declared

444

REFERENCES

1. Poston L, Caleyachetty R, Cnattingius S, Corvalan C, Uauy R, Herring S, Gillman MW. Preconceptional and maternal obesity: epidemiology and health consequences. *The lancet Diabetes & endocrinology* 2016;**4**:1025-1036.

2. Godfrey KM, Reynolds RM, Prescott SL, Nyirenda M, Jaddoe VWV, Eriksson JG, Broekman BFP. Influence of maternal obesity on the long-term health of offspring. *The Lancet Diabetes & Endocrinology*;**5**:53-64.

3. Reynolds RM, Allan KM, Raja EA, Bhattacharya S, McNeill G, Hannaford PC, Sarwar N, Lee AJ, Bhattacharya S, Norman JE. Maternal obesity during pregnancy and premature mortality from cardiovascular event in adult offspring: follow-up of 1 323 275 person years. *Bmj* 2013;**347**:f4539.

4. Fernandez-Twinn DS, Blackmore HL, Siggens L, Giussani DA, Cross CM, Foo R, Ozanne SE. The programming of cardiac hypertrophy in the offspring by maternal obesity is associated with hyperinsulinemia, AKT, ERK, and mTOR activation. *Endocrinology* 2012;**153**:5961-5971.

5. Loche E, Blackmore HL, Carpenter AAM, Beeson JH, Pinnock A, Ashmore TJ, Aiken CE, de Almeida-Faria J, Schoonejans J, Giussani DA, Fernandez-Twinn DS, Ozanne SE. Maternal Diet-Induced Obesity Programmes Cardiac Dysfunction in Male Mice Independently of Post-Weaning Diet. *Cardiovasc Res* 2018;**114**:1372-1384.

6. Ingul CB, Loras L, Tegnander E, Eik-Nes SH, Brantberg A. Maternal obesity affects fetal myocardial function as early as in the first trimester. *Ultrasound in obstetrics & gynecology : the official journal of the International Society of Ultrasound in Obstetrics and Gynecology* 2016;**47**:433-442.

7. Ece İ, Uner A, Balli S, Kibar AE, Oflaz MB, Kurdoglu M. The Effects of Pre-pregnancy Obesity on Fetal Cardiac Functions. *Pediatric Cardiology* 2014;**35**:838-843.

8. Toemen L, Gishti O, van Osch-Gevers L, Steegers EA, Helbing WA, Felix JF, Reiss IK, Duijts L, Gaillard R, Jaddoe VW. Maternal obesity, gestational weight gain and childhood cardiac outcomes: role of childhood body mass index. *International journal of obesity (2005)* 2016;**40**:1070-1078.

9. Fan X, Turdi S, Ford SP, Hua Y, Nijland MJ, Zhu M, Nathanielsz PW, Ren J. Influence of gestational overfeeding on cardiac morphometry and hypertrophic protein markers in fetal sheep. *J Nutr Biochem* 2011;**22**:30-37.

10. Huang Y, Yan X, Zhao JX, Zhu MJ, McCormick RJ, Ford SP, Nathanielsz PW, Ren J, Du M. Maternal obesity induces fibrosis in fetal myocardium of sheep. *Am J Physiol Endocrinol Metab* 2010;**299**:E968-975.

11. Kandadi MR, Hua Y, Zhu M, Turdi S, Nathanielsz PW, Ford SP, Nair S, Ren J. Influence of gestational overfeeding on myocardial proinflammatory mediators in fetal sheep heart. *J Nutr Biochem* 2013;**24**:1982-1990.

12. Wang J, Ma H, Tong C, Zhang H, Lawlis GB, Li Y, Zang M, Ren J, Nijland MJ, Ford SP, Nathanielsz PW, Li J. Overnutrition and maternal obesity in sheep pregnancy alter the JNK-IRS-1 signaling cascades and cardiac function in the fetal heart. *Faseb j* 2010;**24**:2066-2076.

13. Rosario FJ, Kanai Y, Powell TL, Jansson T. Increased placental nutrient transport in a novel mouse model of maternal obesity with fetal overgrowth. *Obesity* 2015;**23**:1663-1670.

14. Acosta O, Ramirez VI, Lager S, Gaccioli F, Dudley DJ, Powell TL, Jansson T. Increased glucose and placental GLUT-1 in large infants of obese nondiabetic mothers. *Am J Obstet Gynecol* 2015;**212**:227.e221-227.

15. Powell TL, Barner K, Madi L, Armstrong M, Manke J, Uhlson C, Jansson T, Ferchaud-Roucher V. Sex-specific responses in placental fatty acid oxidation, esterification and transfer capacity to maternal obesity. *Biochim Biophys Acta Mol Cell Biol Lipids* 2021;**1866**:158861.

16. Gázquez A, Prieto-Sánchez MT, Blanco-Carnero JE, Ruíz-Palacios M, Nieto A, van Harskamp D, Oosterink JE, Schierbeek H, van Goudoever JB, Demmelmair H, Koletzko B, Larqué E. Altered materno-fetal transfer of 13C-polyunsaturated fatty acids in obese pregnant women. *Clin Nutr* 2020;**39**:1101-1107.

17. Mdaki KS, Larsen TD, Wachal AL, Schimelpfenig MD, Weaver LJ, Dooyema SD, Louwagie EJ, Baack ML. Maternal high-fat diet impairs cardiac function in offspring of diabetic pregnancy through metabolic stress and mitochondrial dysfunction. 2016;**310**:H681-692.

18. Turdi S, Ge W, Hu N, Bradley KM, Wang X, Ren J. Interaction between maternal and postnatal high fat diet leads to a greater risk of myocardial dysfunction in offspring via enhanced lipotoxicity, IRS-1 serine phosphorylation and mitochondrial defects. *Journal of Molecular and Cellular Cardiology* 2013;**55**:117-129.

19. Rijzewijk LJ, van der Meer RW, Lamb HJ, de Jong HW, Lubberink M, Romijn JA, Bax JJ, de Roos A, Twisk JW, Heine RJ, Lammertsma AA, Smit JW, Diamant M. Altered myocardial substrate metabolism and decreased diastolic function in nonischemic human diabetic cardiomyopathy: studies with cardiac positron emission tomography and magnetic resonance imaging. *Journal of the American College of Cardiology* 2009;**54**:1524-1532.

20. Herrero P, Peterson LR, McGill JB, Matthew S, Lesniak D, Dence C, Gropler RJ. Increased myocardial fatty acid metabolism in patients with type 1 diabetes mellitus. *Journal of the American College of Cardiology* 2006;**47**:598-604.

21. Son N-H, Park T-S, Yamashita H, Yokoyama M, Huggins LA, Okajima K, Homma S, Szabolcs MJ, Huang L-S, Goldberg IJ. Cardiomyocyte expression of PPARγ leads to cardiac dysfunction in mice. *The Journal of Clinical Investigation* 2007;**117**:2791-2801.

22. Aye IL, Rosario FJ, Powell TL, Jansson T. Adiponectin supplementation in pregnant mice prevents the adverse effects of maternal obesity on placental function and fetal growth. *Proc Natl Acad Sci U S A* 2015;**112**:12858-12863.

23. Vaughan OR, Rosario FJ, Powell TL, Jansson T. Normalisation of circulating adiponectin levels in obese pregnant mice prevents cardiac dysfunction in adult offspring. *International journal of obesity (2005)* 2019.

24. Haberland M, Montgomery RL, Olson EN. The many roles of histone deacetylases in development and physiology: implications for disease and therapy. *Nature Reviews Genetics* 2009;**10**:32.

25. Alrob OA, Sankaralingam S, Ma C, Wagg CS, Fillmore N, Jaswal JS, Sack MN, Lehner R, Gupta MP, Michelakis ED, Padwal RS, Johnstone DE, Sharma AM, Lopaschuk GD. Obesity-induced lysine acetylation increases cardiac fatty acid oxidation and impairs insulin signalling. *Cardiovasc Res* 2014;**103**:485-497.

26. Hacker A, Capel B, Goodfellow P, Lovell-Badge R. Expression of Sry, the mouse sex determining gene. *Development* 1995;**121**:1603-1614.

27. Zheng X, Wen L, Yu S-J, Huang S-C, Feng DD. A study of non-invasive Patlak quantification for whole-body dynamic FDG-PET studies of mice. *Biomed Signal Process Control* 2012;**7**:438-446.

28. Kuznetsov AV, Veksler V, Gellerich FN, Saks V, Margreiter R, Kunz WS. Analysis of mitochondrial function in situ in permeabilized muscle fibers, tissues and cells. *Nat Protoc* 2008;**3**:965-976.

29. Son NH, Basu D, Samovski D, Pietka TA, Peche VS, Willecke F, Fang X, Yu SQ, Scerbo D, Chang HR, Sun F, Bagdasarov S, Drosatos K, Yeh ST, Mullick AE, Shoghi KI, Gumaste N, Kim K, Huggins LA, Lhakhang T, Abumrad NA, Goldberg IJ. Endothelial cell CD36 optimizes tissue fatty acid uptake. *J Clin Invest* 2018;**128**:4329-4342.

30. Suter MA, Chen A, Burdine MS, Choudhury M, Harris RA, Lane RH, Friedman JE, Grove KL, Tackett AJ, Aagaard KM. A maternal high-fat diet modulates fetal SIRT1 histone and protein deacetylase activity in nonhuman primates. *The FASEB Journal* 2012;**26**:5106-5114.

31. McCurdy CE, Schenk S, Hetrick B, Houck J, Drew BG, Kaye S, Lashbrook M, Bergman BC, Takahashi DL, Dean TA, Nemkov T, Gertsman I, Hansen KC, Philp A, Hevener AL, Chicco AJ, Aagaard KM, Grove KL, Friedman JE. Maternal obesity reduces oxidative capacity in fetal skeletal muscle of Japanese macaques. *JCI insight* 2016;**1**:e86612.

32. Vidal-Puig A, Jimenez-Liñan M, Lowell BB, Hamann A, Hu E, Spiegelman B, Flier JS, Moller DE. Regulation of PPAR gamma gene expression by nutrition and obesity in rodents. *The Journal of clinical investigation* 1996;**97**:2553-2561.

33. Diaz P, Harris J, Rosario FJ, Powell TL, Jansson T. Increased placental fatty acid transporter 6 and binding protein 3 expression and fetal liver lipid accumulation in a mouse model of obesity in pregnancy. *Am J Physiol Regul Integr Comp Physiol* 2015;**309**:R1569-1577.

34. Vaduganathan M, Patel RB, Michel A, Shah SJ, Senni M, Gheorghiade M, Butler J. Mode of Death in Heart Failure With Preserved Ejection Fraction. *Journal of the American College of Cardiology* 2017;**69**:556-569.

35. Wang YC, Xiao XL, Li N, Yang D, Xing Y, Huo R, Liu MY, Zhang YQ, Dong DL. Oestrogen inhibits BMP4-induced BMP4 expression in cardiomyocytes: a potential mechanism of oestrogen-mediated protection against cardiac hypertrophy. *British Journal of Pharmacology* 2015;**172**:5586-5595.

36. Nelson JF, Felicio LS, Osterburg HH, Finch CE. Altered profiles of estradiol and progesterone associated with prolonged estrous cycles and persistent vaginal cornification in aging C57BL/6J mice. *Biol Reprod* 1981;**24**:784-794.

37. Nelson JF, Felicio LS, Randall PK, Sims C, Finch CE. A longitudinal study of estrous cyclicity in aging C57BL/6J mice: I. Cycle frequency, length and vaginal cytology. *Biol Reprod* 1982;**27**:327-339.

38. Ho KKL, Pinsky JL, Kannel WB, Levy D. The epidemiology of heart failure: The Framingham Study. *Journal of the American College of Cardiology* 1993;**22**:A6-A13.

39. Kadkhodayan A, Lin CH, Coggan AR, Kisrieva-Ware Z, Schechtman KB, Novak E, Joseph SM, Davila-Roman VG, Gropler RJ, Dence C, Peterson LR. Sex affects myocardial blood flow and fatty acid substrate metabolism in humans with nonischemic heart failure. *Journal of nuclear cardiology : official publication of the American Society of Nuclear Cardiology* 2017;**24**:1226-1235.

40. Peterson LR, Soto PF, Herrero P, Schechtman KB, Dence C, Gropler RJ. Sex Differences in Myocardial Oxygen and Glucose Metabolism. *Journal of nuclear cardiology : official publication of the American Society of Nuclear Cardiology* 2007;**14**:573-581.

41. Iozzo P, Chareonthaitawee P, Dutka D, Betteridge DJ, Ferrannini E, Camici PG. Independent association of type 2 diabetes and coronary artery disease with myocardial insulin resistance. *Diabetes* 2002;**51**:3020-3024.

42. Cole MA, Murray AJ, Cochlin LE, Heather LC, McAleese S, Knight NS, Sutton E, Jamil AA, Parassol N, Clarke K. A high fat diet increases mitochondrial fatty acid oxidation and uncoupling to decrease efficiency in rat heart. *Basic research in cardiology* 2011;**106**:447-457.

43. Guzzardi MA, Liistro T, Gargani L, Ait Ali L, D'Angelo G, Rocchiccioli S, La Rosa F, Kemeny A, Sanguinetti E, Ucciferri N, De Simone M, Bartoli A, Festa P, Salvadori PA, Burchielli S, Sicari R, Iozzo P. Maternal Obesity and Cardiac Development in the Offspring: Study in Human Neonates and Minipigs. *JACC Cardiovasc Imaging* 2018;**11**:1750-1755.

44. Mikkelsen TS, Xu Z, Zhang X, Wang L, Gimble JM, Lander ES, Rosen ED. Comparative epigenomic analysis of murine and human adipogenesis. *Cell* 2010;**143**:156-169.

45. Aagaard-Tillery KM, Grove K, Bishop J, Ke X, Fu Q, McKnight R, Lane RH. Developmental origins of disease and determinants of chromatin structure: maternal diet modifies the primate fetal epigenome. *Journal of Molecular Endocrinology* 2008;**41**:91-102.

46. Robinson MD, Oshlack A. A scaling normalization method for differential expression analysis of RNA-seq data. *Genome Biology* 2010;**11**:R25.

585   47.   Benjamini Y, Hochberg Y. Controlling the False Discovery Rate: A Practical and Powerful Approach
586   to Multiple Testing. *Journal of the Royal Statistical Society: Series B (Methodological)* 1995;**57**:289-
587   300.
588   48.   Ferchaud-Roucher V, Rudolph MC, Jansson T, Powell TL. Fatty acid and lipid profiles in primary
589   human trophoblast over 90h in culture. *Prostaglandins, leukotrienes, and essential fatty acids*
590   2017;**121**:14-20.
591   49.   Matyash V, Liebisch G, Kurzchalia TV, Shevchenko A, Schwudke D. Lipid extraction by methyl-tert-
592   butyl ether for high-throughput lipidomics. *Journal of lipid research* 2008;**49**:1137-1146.
593   50.   Harrison KA, Bergman BC. HPLC-MS/MS Methods for Diacylglycerol and Sphingolipid Molecular
594   Species in Skeletal Muscle. *Methods Mol Biol* 2019;**1978**:137-152.

595

596

597 **Table 1 Effect of maternal obesity on body and heart weights in E18.5 fetuses**

	Con	Ob	P value (t test)
Males	n=5 litters	n=5 litters	
Body weight (g)	1050 ± 50	1272 ± 26	**0.004***
Heart weight (mg)	4.84 ± 0.56	7.64 ± 0.28	**0.002***
Females	n=5 litters	n=5 litters	
Body weight (g)	995 ± 43	1228 ± 58	**0.012***
Heart weight (mg)	3.88 ± 0.26	7.14 ± 0.32	**<0.001***

598

599 Body and heart weights, determined at necropsy, in male and female fetuses of control (Con) and obese
600 (Ob) dams. Litter mean values for Con and Ob groups compared by Student's t-test. *, P<0.05. Mean ±
601 SEM.

602

603 **Table 2 Effect of maternal obesity on body and heart weights in 6-month-old adult offspring**

	Con	Ob	P value (t test)
Males	n=47	n=31	
Body weight (g)	36.4 ± 0.9	36.1 ± 1.1	0.830
Heart weight (mg)	158 ± 3	162 ± 5	0.527
(% body wt. x 1000)	4.40 ± 0.10	4.55 ± 0.16	0.405
LV weight (g)	112 ± 2	114 ± 4	0.623
(% body wt. x 1000)	3.08 ± 0.07	3.24 ± 0.16	0.289
Females	n=42	n=34	
Body weight (g)	26.8 ± 0.7	28.5 ± 0.9	0.149
Heart weight (mg)	127 ± 3	139 ± 4	0.012*
(% body wt. x 1000)	4.79 ± 0.10	4.97 ± 0.16	0.305
LV weight (g)	89.7 ± 2.4	93.9 ± 3.54	0.325
(% body wt. x 1000)	3.35 ± 0.06	3.44 ± 0.13	0.561

604

605 Body, heart and LV weight, determined at necropsy, in 6-month old male and female offspring of control
606 (Con) and obese (Ob) dams. Con and Ob groups compared by Student's t-test. *, P<0.05. Mean ± SEM.

607 **Table 3 Effect of maternal obesity on cardiac fatty acid and glucose transporter expression in 6-**
608 **month-old adult offspring**

	Con	Ob	P value (t test)
Males	n=10	n=10	
CD36	1.00 ± 0.05	1.02 ± 0.06	0.748
FATP1	1.00 ± 0.23	0.90 ± 0.32	0.331[b]
FATP6	1.00 ± 0.24	1.25 ± 0.28	0.501
GLUT1	1.00 ± 0.10	1.18 ± 0.15	0.321
GLUT4	1.00 ± 0.12	1.12 ± 0.11	0.448
Females	n=10	n=10	
CD36	1.00 ± 0.05	0.95 ± 0.06	0.462
FATP1	1.00 ± 0.18	2.27 ± 0.67	0.143[a]
FATP6	1.00 ± 0.17	0.44 ± 0.06	**0.006[b]***
GLUT1	1.00 ± 0.32	0.88 ± 0.34	0.310[a]
GLUT4	1.00 ± 0.03	1.02 ± 0.05	0.746

609

610 Relative transporter protein abundance in LV homogenates, determined by western blot, in 6-month old

611 male and female offspring of control (Con) and obese (Ob) dams. Con and Ob groups compared by

612 Student's t-test or Mann-Whitney test[a], as appropriate to distribution. [b]Log transformed prior to

613 statistical analysis. *P<0.05. Mean ± SEM.

614

615 **FIGURE LEGENDS**

616 **Fig. 1 Maternal obesity induces fetal cardiac hypertrophy in association with altered transcription of**
617 **metabolic genes at E18.5.**

618 (A, B) Heart weight, relative to body weight, in female and male fetuses of control (Con) and obese (Ob)
619 dams, on E18.5 of gestation. Con and Ob groups compared by Student's t-test. P and n values given in
620 figure. Bars are mean ± SEM. Symbols represent mean values of all pups of each sex within one litter. (C
621 – F) Top 10 biological processes, ranked by P value, predicted to be inhibited (C, D) or activated (E, F) in
622 hearts of female and male fetuses of obese dams, based on Ingenuity Pathway Analysis of differential
623 gene expression, compared to controls. Activation status determined by z-score >|1.7|. (G) Comparison
624 of biological processes activated or inhibited in response to maternal obesity, in male and female fetuses.
625 Color scale indicates activation z-score relative to control fetuses. (H) Comparison of metabolic genes
626 differentially expressed in response to maternal obesity, in male and female fetuses. Color scale indicates
627 differential expression relative to control fetuses. (I, J) Predicted effect of differentially expressed
628 metabolic genes on downstream biological processes in hearts of female and male fetuses of obese dams.
629 Color of molecules represents expression change Ob vs Con: red, upregulated; green, downregulated.
630 Color of arrows represents direction of predicted effect on downstream processes: orange, activation;
631 grey, neutral; yellow, expression inconsistent with predicted activation. (K, L) Least-squared mean relative
632 PPARG expression in female and male fetal hearts from Con and Ob dams determined by RNASeq (n=5 of
633 each sex per group). P values given in figure.

634 **Fig. 2 Maternal obesity causes age- and sex-dependent left ventricular diastolic dysfunction in adult**
635 **offspring.**

636 Echocardiographic indices of diastolic function in 3- to 24-month old male (A, C, E) and female (B, D, F)
637 offspring of control (white bars) and obese dams (grey bars). (A, B) Ratios of early- to late-diastolic left
638 ventricular wall displacement determined by tissue Doppler (E'/A'). (C, D) Ratios of early- to late-diastolic
639 mitral inflow determined by pulsed wave Doppler (E/A). (E, F) Ratio of early diastolic mitral inflow to wall
640 displacement (E/E'). Main effects of maternal obesity and postnatal age, and their interaction, were
641 determined by two-way ANOVA and P values given in figure. Post-hoc comparisons of Con and Ob groups
642 at each age used the Sidak test; * P<0.05, ** P<0.01, ***P<0.001. Bars are mean ± SEM. Symbols represent
643 individual animals. n values given in bars.

644 **Fig. 3 Maternal obesity causes age- and sex-dependent left ventricular dilatation in adult offspring.**

645 Left ventricular end-diastolic and end-systolic volumes, determined by echocardiography, in 3- to 24-
646 month old male (A, C) and female (B, D) offspring of control (white bars) and obese dams (grey bars). Main
647 effects of maternal obesity and postnatal age, and their interaction, were determined by two-way ANOVA
648 and P values given in figure. Post-hoc comparisons of Con and Ob groups at each age used the Sidak test;
649 * P<0.05, ** P<0.01, ***P<0.001 Bars are mean ± SEM. Points represent individual animals. n values given
650 in figure.

651 **Fig. 4 Maternal obesity increases cardiac expression of Pparg and its downstream targets in adult**
652 **offspring.**

653 Relative expression of candidate genes in left ventricles of 6-month old old male (A, Con n=11, Ob n=10)
654 and female (B, Con n=9, Ob n=10) offspring at age 6 months, determined by qPCR relative to *Rna18s* and
655 *Rps29*. Bars are mean ± SEM. Con and Ob offspring compared by Student's t-test.*, P<0.05. (C, D)
656 Correlation of left ventricular *Pparg* expression with E/E' ratio in male offspring and end-diastolic volume
657 in female offspring of Con and Ob dams. Relationship between variables assessed by Pearson's
658 correlation, P, R and N values given in figure. Least-squares regression line shown.

659 **Fig. 5 Maternal obesity increases myocardial fatty acid oxidation in adult male, but not female, offspring**

660 (A, B) In vivo left ventricular 3H-oleic acid clearance in male (Con n=7, Ob n=4) and female (Con n=3, Ob
661 n=6) offspring. (C, D) Palmitoyl carnitine-supported mitochondrial respiration rates in isolated,
662 permeabilized cardiac myofibers from 6-month old male (Con n=16, Ob n=10) and female (Con n=16, Ob
663 n=9) offspring of Con and Ob dams. Respiration rates and clearances compared between Con and Ob
664 groups by Student's t-test, P values given in figure. Mean ± SEM. Symbols represent individual offspring.
665 (E) Correlation between palmitoyl carnitine supported coupling control ratio and Pparg expression in male
666 offspring. Relationship between variables determined by Pearson's correlation, P and R values in figure.
667 Least-squares regression line shown.

668 **Fig. 6 Maternal obesity impairs myocardial glucose uptake in adult female, but not male, offspring**

669 (A-D) Left ventricular 8F-fluorodeoxyglucose clearance in male (Con n=8, Ob n=9) and female (Con n=10,
670 Ob n=11) offspring of control and obese dams at age 6 months. Con and Ob groups compared by least-
671 square linear regression of (A, C) Patlak plot, symbols represent mean ± SEM values for all individuals
672 within each group, at each normalized time point. (B, D) Histogram of mean ± SEM clearance (gradient of
673 Patlak plot) for each experimental group. (E, F) Pyruvate-supported mitochondrial respiration rates in
674 isolated, permeabilized cardiac myofibers from 6-month old male (Con n=16, Ob n=10) and female (Con

675   n=15, Ob n=9) offspring of control and obese dams. Con and Ob groups compared by Student's t test. P

676   values for intergroup comparisons given in figure. Bars are mean + SEM. Points represent individual

677   animals.

678   **Fig. 7 Maternal obesity does not affect myocardial histone H3 acetylation in adult offspring.**

679   Relative protein abundance of total (A, B), acetyl-lysine-27 (C, D) and acetyl-lysine-9 (E, F) histone H3 in

680   6-month old male and female offspring of Con and Ob dams. Con and Ob groups compared by Student's

681   t-test, P values given in figure. Bars are mean ± SEM. Points represent individual animals. n values given
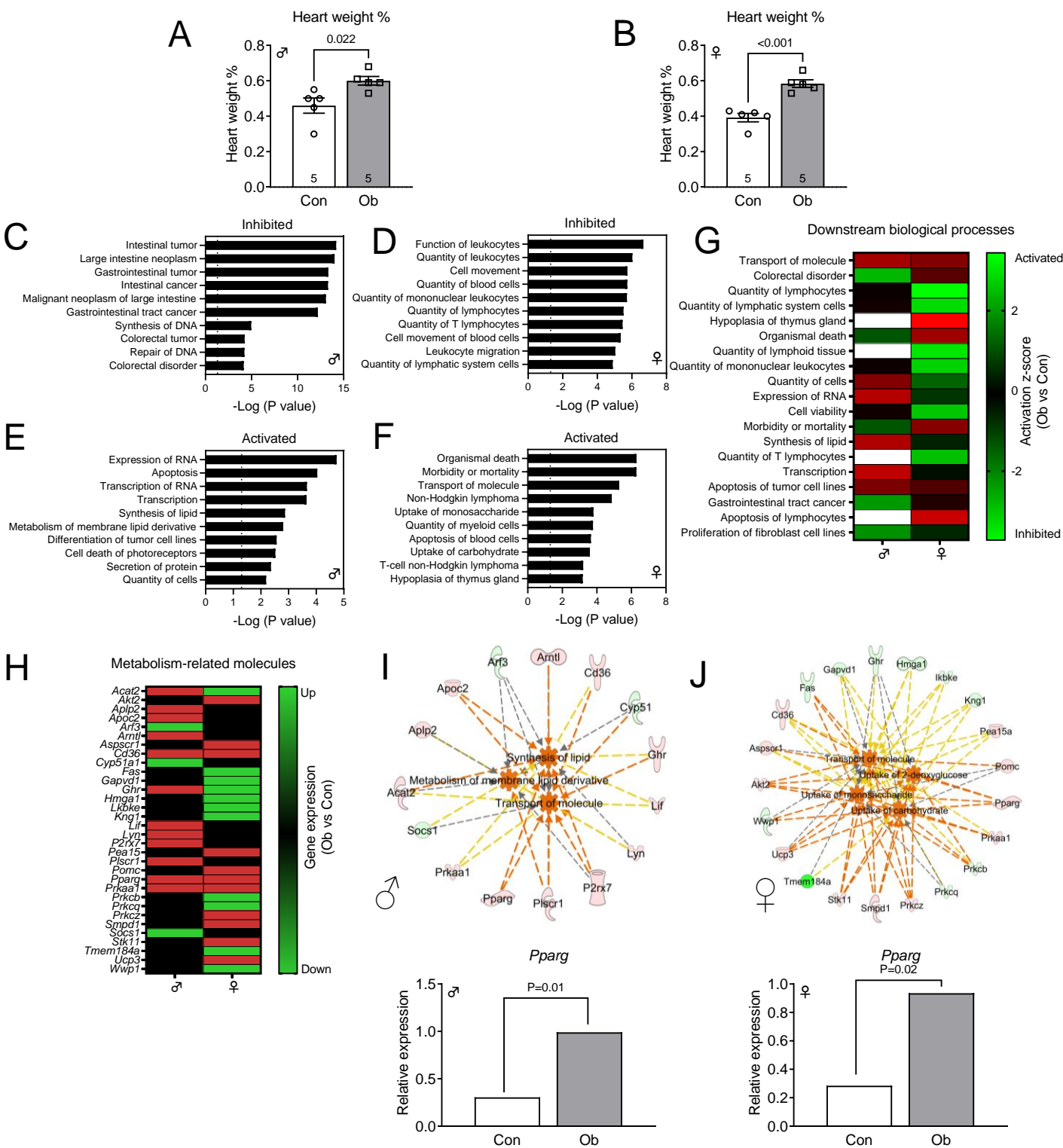
682   in figure.

Fig. 1 Maternal obesity induces fetal cardiac hypertrophy in association with altered transcription of metabolic genes at E18.5.

Fig. 2 Maternal obesity causes age- and sex-dependent left ventricular diastolic dysfunction in adult offspring. ○ Control □ Obese
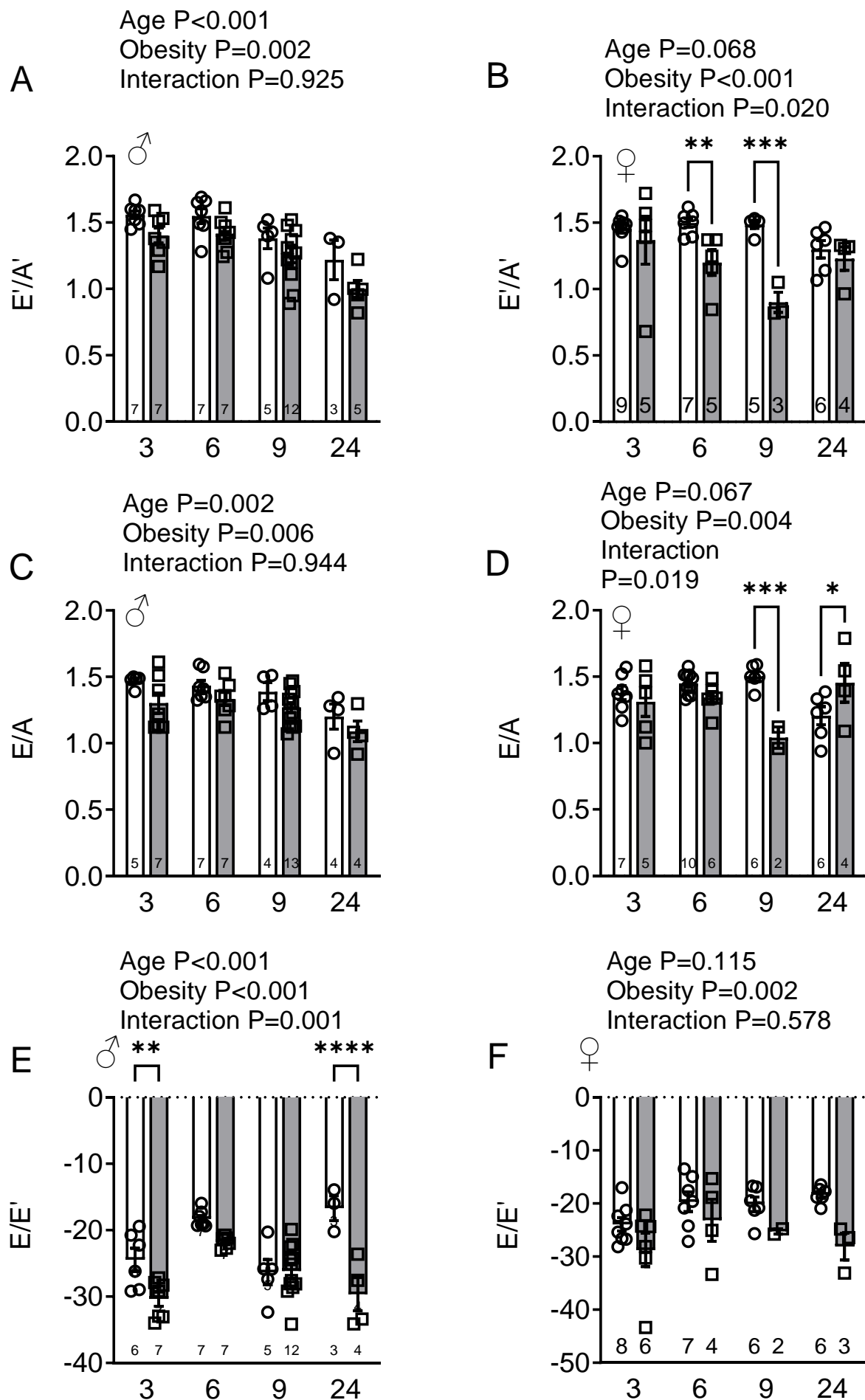
Fig. 3 Maternal obesity causes age- and sex-dependent left ventricular dilatation in adult offspring.

Fig. 4 Maternal obesity increases cardiac expression of Pparg and its downstream targets in adult offspring.

Fig. 5 Maternal obesity increases myocardial fatty acid oxidation in adult male, but not female, offspring

Fig. 6 Maternal obesity impairs myocardial glucose uptake in adult female, but not male, offspring

Fig. 7 Maternal obesity does not affect myocardial histone H3 acetylation in adult offspring.

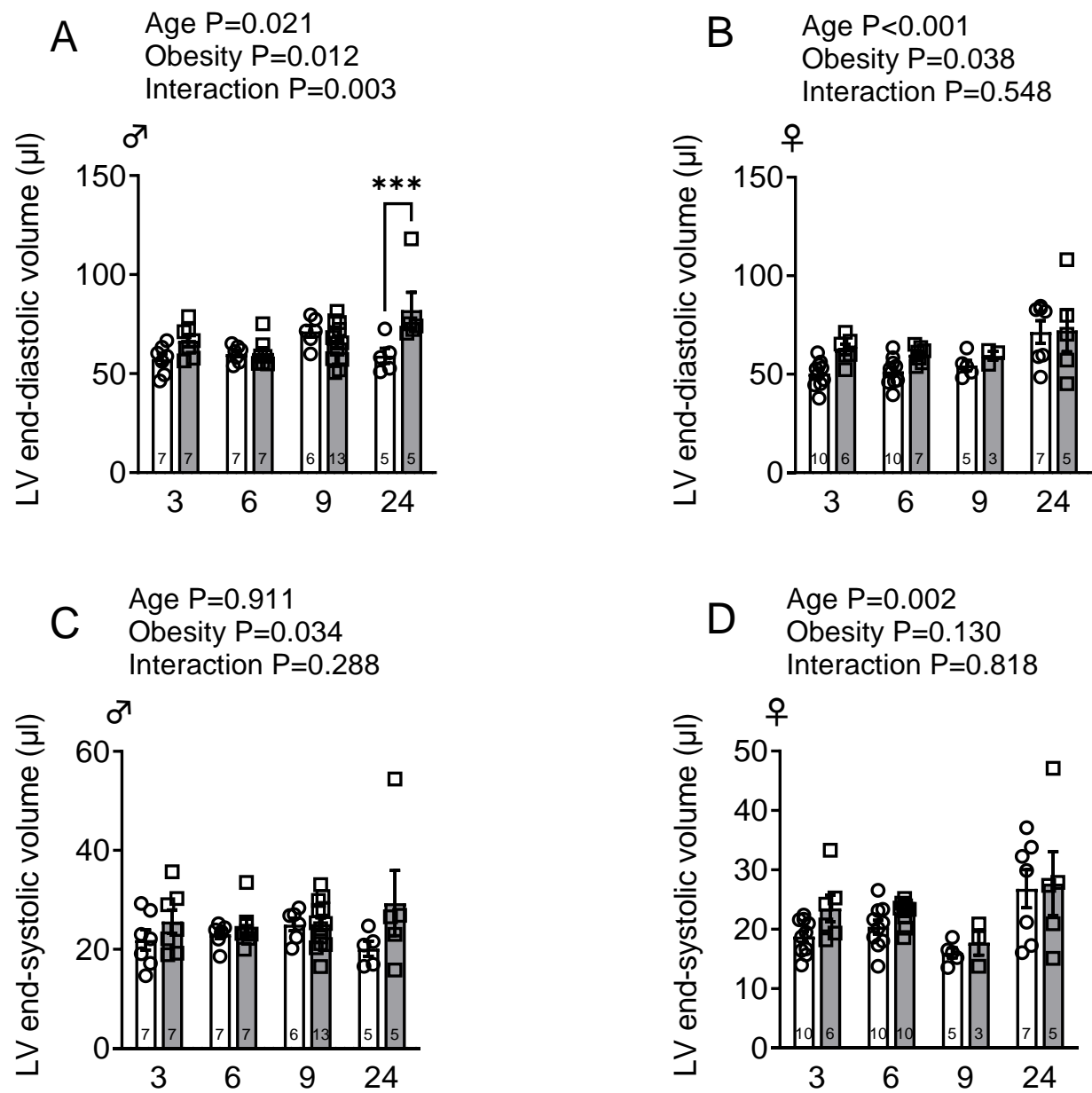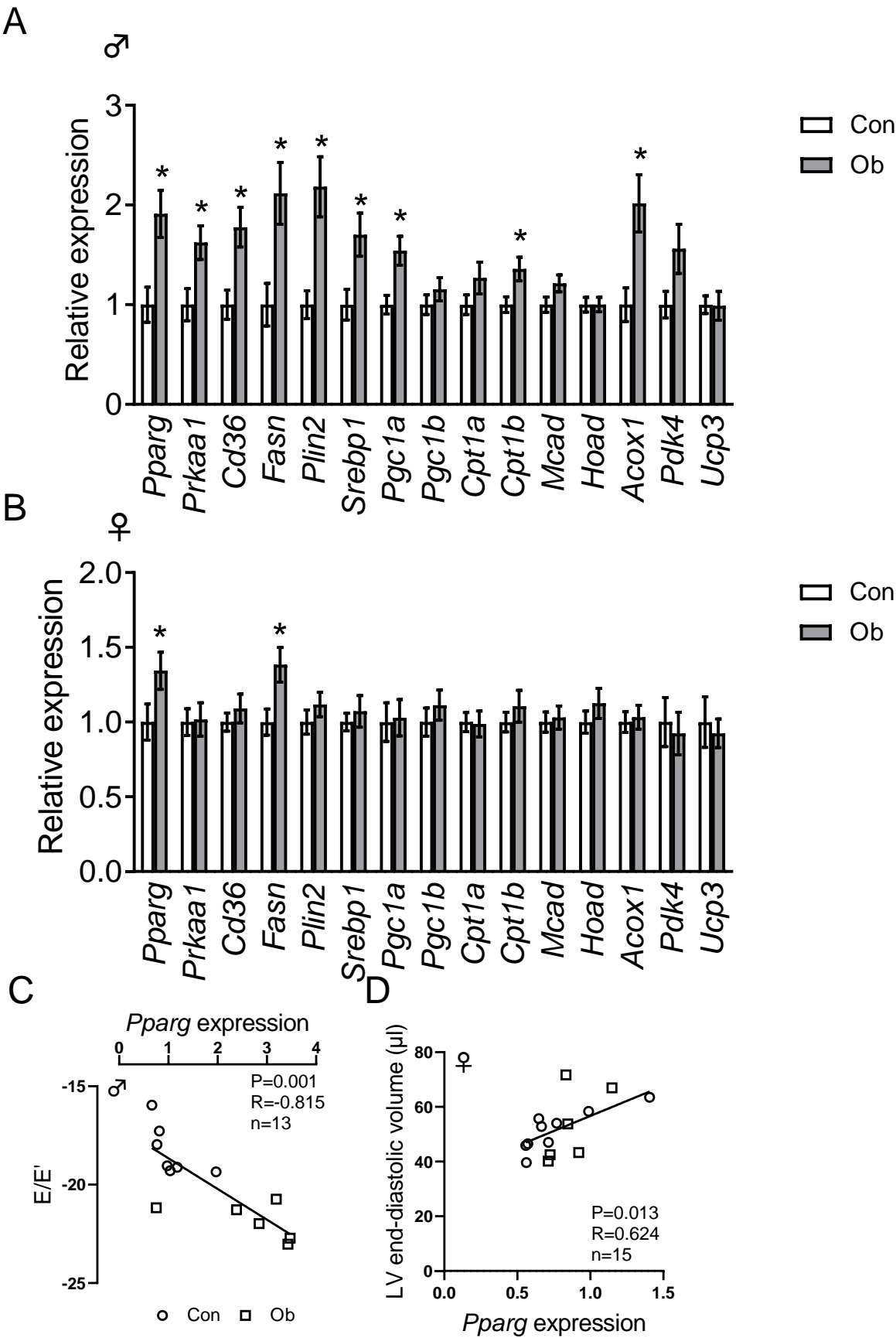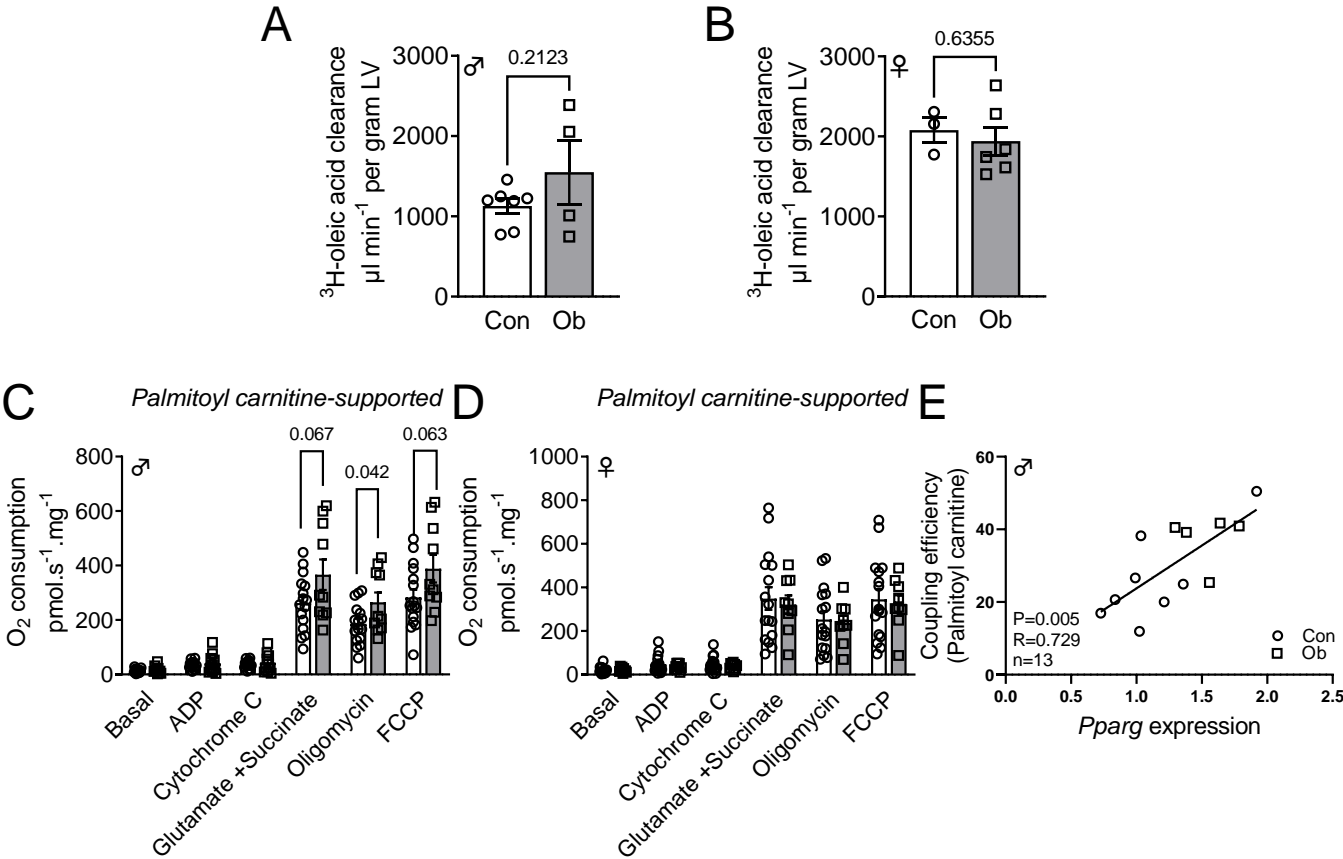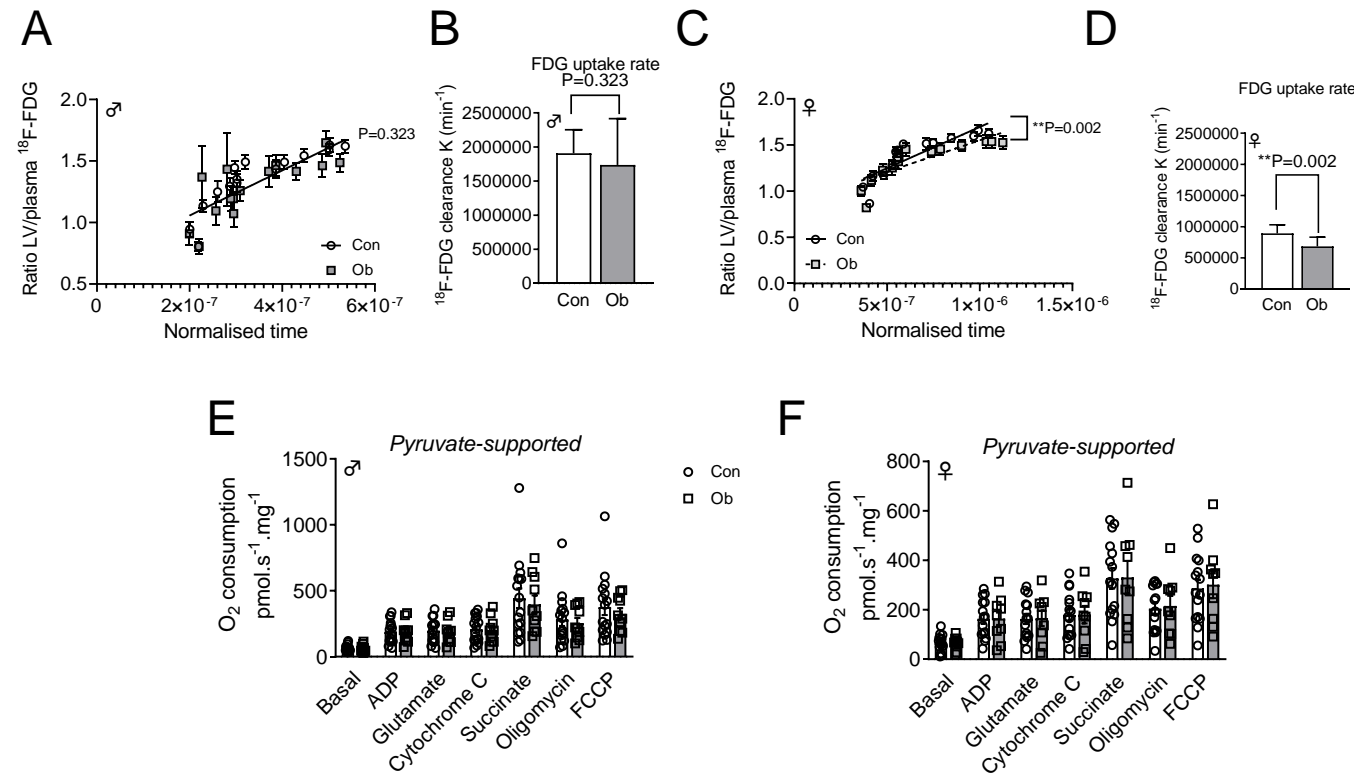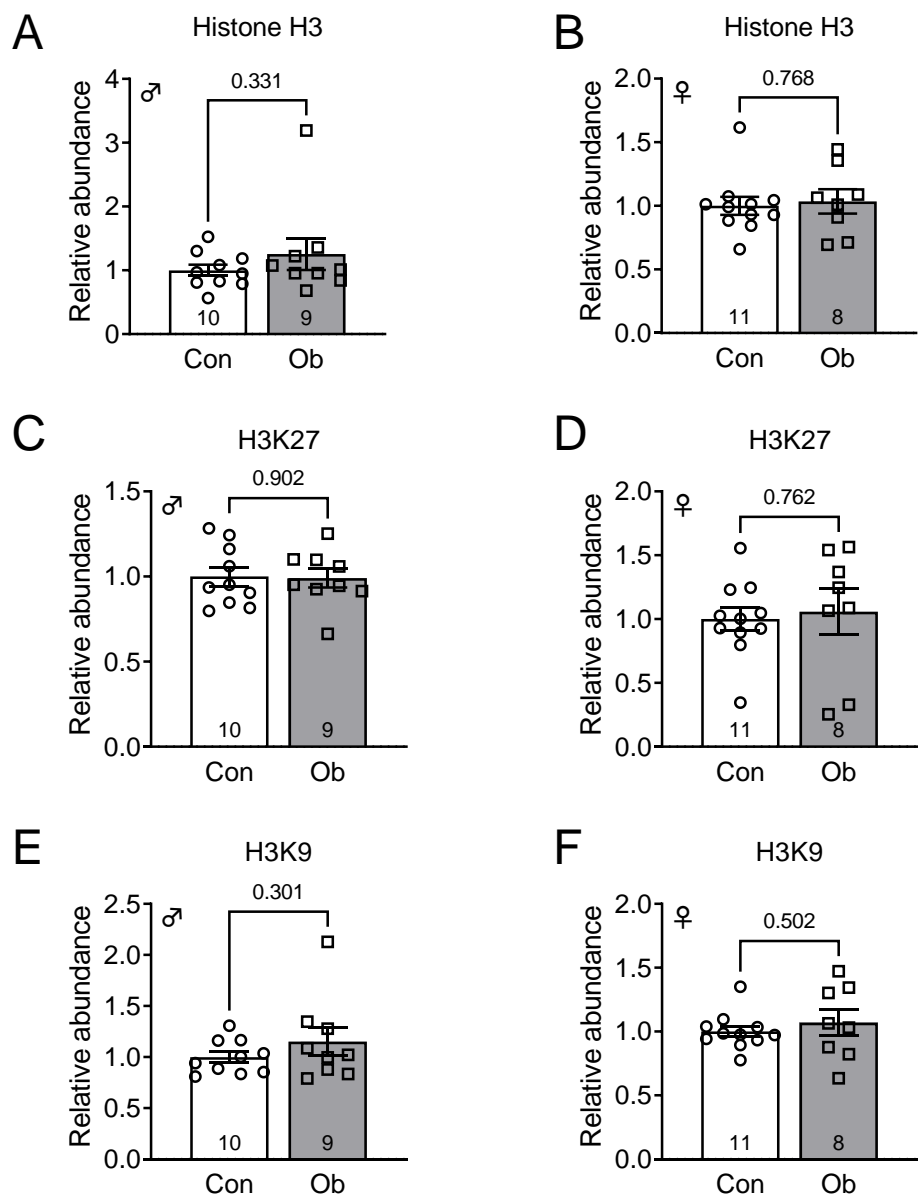1   **SUPPLEMENTARY MATERIAL**

2

3   **MATERNAL OBESITY CAUSES FETAL CARDIAC HYPERTROPHY AND ALTERS ADULT OFFSPRING**
4   **MYOCARDIAL METABOLISM IN MICE**

5

6   Owen R. Vaughan[1], Fredrick J. Rosario[1], Jeannie Chan[2], Laura A. Cox[2], Veronique Ferchaud-Roucher[1], Karin
7   A. Zemski-Berry[3], Jane E.B. Reusch[3], Amy C. Keller[3], Theresa L. Powell[1,4] and Thomas Jansson[1]

8   [1]Department of Obstetrics and Gynecology, University of Colorado Anschutz Medical Campus, Aurora, CO,
9   USA

10   [2]Department of Molecular Medicine, Wake Forest School of Medicine, Winston-Salem, NC, USA

11   [3]Department of Medicine, Division of Endocrinology, Metabolism and Diabetes, University of Colorado
12   Anschutz Medical Campus, Aurora, CO, USA and Rocky Mountain Regional VA Medical Center, Aurora, CO,
13   USA

14   [4]Department of Pediatrics, University of Colorado Anschutz Medical Campus, Aurora, CO, USA

15

16   **Short title:** Maternal obesity alters offspring heart metabolism

17   **Manuscript category:** Original article

18   **Correspondence:**

19   Owen R. Vaughan, PhD

20   Department of Obstetrics and Gynecology

21   University of Colorado Anschutz Medical Campus

22   12700 E19th Avenue

23   Aurora, CO, USA

24   owen.vaughan@CUAnschutz.edu

25   Phone: (303) 724-8622

26   Fax: (303) 724-3512

1

27 **SUPPLEMENTARY TABLES**

28 **Suppl. Table 1 Primer sequences used for qRT- PCR analysis of adult offspring hearts**

Target mRNA	Forward primer sequence	Reverse primer sequence	Source reference
Pparg	GAGTGTGACGACAAGATTTG	GGTGGGCCAGAATGGCATCT	PMID: 25157099
Cd36	AATGGCACAGACGCAGCCT	GGTTGTCTGGATTCTGGA	PMID: 25157099
Prkaa1	GTCAAAGCCGACCCAATGATA	CGTACACGCAAATAATAGGGGTT	PMID: 31409640
Pgc1a	TGTTCCCGATCACCATATTCC	TCCCGCTTCTCGTGCTCTTT	PMID: 22932259
Pgc1b	AGGTGTTCGGTGAGATTGTA	TCAGATGTGGGATCATAGTCA	PMID: 22932260
Cpt1a	CTCAGTGGGAGCGACTCTTCA	GGCCTCTGTGGTACACGACAA	PMID: 22932258
Cpt1b	TTCAACACTACACGCATCCC	GCCCTCATAGAGCCAGACC	PMID: 22932257
Mcad	GATGCATCACCCTCGTGTAAC	AAGCCCTTTTCCCCTGAAG	PMID: 23349477
Hoad	GCAAAATCCAAGAAGGGAATTG	TGGTTGAAAGGCAGCTCAG	PMID: 21990309
Pdk4	CCGCTGTCCATGAAGCA	GCAGAAAAGCAAAGGACGTT	PMID: 16314495
Ucp3	CCAACATCACAAGAAATGC	TACAAACATCATCACGTTCC	PMID: 12351640

29

30

31 **Suppl. Table 3 Effect of maternal obesity on mitochondrial coupling efficiency in adult offspring**

	Con	Ob	P value (t test)
Males	n=16	n=10	
Palmitoyl-carnitine supported respiration	33.4 ± 2.0	31.5 ± 3.6	0.625
Pyruvate-supported respiration	26.8 ± 7.5	23.2 ± 6.1	0.218
Females	n=15	n=9	
Palmitoyl-carnitine supported respiration	29.0 ± 1.6	27.0 ± 2.3	0.475
Pyruvate-supported respiration	28.4 ± 8.0	28.9 ± 8.1	0.871

32 Coupling efficiencies for each of the two combinations of substrates was calculated as 1 minus the
33 ratio (leak state respiration/maximal electron transport chain capacity).

34   **Suppl. Table 4. Effect of maternal obesity on adult offspring myocardial fatty acid content.**

nmol/mg protein	Con	Ob	P value (t-test)
Males	n=10	n=10	
12:0	17.8 ± 8.7	6.9 ± 4.7	0.991
14:0	50.1 ± 28.3	55.0 ± 31.0	1.000
16:0	1983.0± 424.3	1984.0 ± 432.4	1.000
16:1 n-7	16.6 ± 1.5	17.3 ± 6.0	1.000
18:0	1970.0 ± 264.7	2025.0 ± 227.0	1.000
18:1 n-9	1095.0 ± 121.6	1037.0 ± 189.8	1.000
18:2 n-6	4971.0 ± 615.8	4790.0 ± 405.0	1.000
18:3 n-3	7.3 ± 0.7	6.6 ± 0.5	0.999
18:3 n-6	0.01 ± 0.01	0.01 ± 0.004	1.000
20:1 n-9	62.7 ± 6.3	63.3 ± 3.4	1.000
20:3 n-6	73.2 ± 6.6	66.9 ± 3.6	0.999
20:4 n-6	1666.0 ± 148.6	1745.0 ± 79.8	1.000
20:5 n-3	8.9 ± 10.1	15.5 ± 12.3	1.000
22:4 n-6	81.9 ± 8.0	59.9 ± 6.1	0.496
22:5 n-3	255.8 ± 28.5	185.3 ± 12.4	0.460
22:6 n-3	2927.0 ± 224.4	2547.0 ± 192.4	0.973
22:5 n-6	270.7 ± 18.8	255.3 ± 10.2	0.999
Total fatty acids	15463 ± 1554	14859 ± 1288	0.768
Females	n=10	n=10	
12:0	14.2 ± 9.1	0.9 ± 4.1	0.981
14:0	91.4 ± 57.3	3.8 ± 14.4	0.875
16:0	2183.0 ± 709.7	1064.0 ± 244.6	0.113
16:1 n-7	15.8 ± 5.1	14.1 ± 2.6	0.996
18:0	2394 ± 350.3	1817.0 ± 148.6	0.644
18:1 n-9	1181.0 ± 358.8	746.6 ± 155.3	0.595
18:2 n-6	5859.0 ± 391.5	5489.0 ± 423.3	0.195
18:3 n-3	9.9 ± 1.4	8.9 ± 0.8	0.999
18:3 n-6	27.4 ± 18.1	17.4 ± 22.7	0.985
20:1 n-9	55.7 ± 6.0	38.8± 3.9	0.982
20:3 n-6	54.0 ± 2.2	48.1 ± 3.6	1.000
20:4 n-6	1936.0 ± 99.2	1679.0 ± 87.3	0.998
20:5 n-3	20.5 ± 19.6	-14.7 ± 9.4	0.929
22:4 n-6	68.2 ± 3.3	65.9 ± 5.3	0.991
22:5 n-3	138.6 ± 9.9	131.8 ± 8.5	0.986
22:6 n-3	3008.0 ± 226.9	2732.0 ± 204.2	0.850
22:5 n-6	213.2 ± 11.2	212.9 ± 17.5	0.947
Total fatty acids	17269 ± 1641	14055 ± 1083	0.120

35   Fatty acid content, determined by GC/MS, in LV homogenates from 6-month old male and female
36   offspring of control (Con) and obese (Ob) dams. Con and Ob groups compared by Student's t-test
37   with Holm-Sidak multiplicity correction. *P<0.05. Mean ± SEM.

38 **Suppl. Table 5. Effect of maternal obesity on adult offspring myocardial DAG content.**

39

pmol/mg protein	Con	Ob	P value (t-test)
Males	n=6	n=5	
1,2-16:0/18:0DG	7.1 ± 2.1	5.1 ± 1.2	0.997
1,2-16:0/18:1DG	34.3 ± 13.8	12.2 ± 3.3	0.434
1,2-16:0/18:2DG	22.4 ± 9.3	8.3 ± 3.4	0.881
1,2-16:0/20:4DG	4.4 ± 2.1	1.8 ± 1.5	0.997
1,2-1,2-16:0/22:6DG	11.7 ± 3.9	5.3 ± 2.9	0.997
1,2-18:0/18:1DG	9.4 ± 4.0	2.2 ± 0.8	0.997
1,2-18:0/18:2DG	12.7 ± 4.0	6.8 ± 1.8	0.997
1,2-18:0/20:4DG	55.1 ± 12.8	25.9 ± 6.3	0.128
1,2-18:0/22:6DG	9.7 ± 3.3	3.9 ± 1.4	0.997
1,2-18:2/18:1DG	**52.3 ± 21.9**	**17.5 ± 4.7**	0.033
1,2-di16:0DGa	12.3 ± 3.5	5.4 ± 0.9	0.997
1,2-di18:0DGa	5.2 ± 2.4	0.8 ± 0.5	0.997
1,2-di18:1DGa	34.4 ± 16.2	7.0 ± 2.3	0.178
1,2-di18:2DGa	28.0 ± 9.7	12.0 ± 4.1	0.816
Total DAGs	305 ± 105	115 ± 32	0.084[b]
Females	n=8	n=6	
1,2-16:0/18:0DG	9.7 ± 1.6	9.8 ± 1.8	1.000
1,2-16:0/18:1DG	35.4 ± 7.1	29.6 ± 4.7	0.997
1,2-16:0/18:2DG	23.7 ± 5.4	19.0 ± 3.1	0.997
1,2-16:0/20:4DG	5.5 ± 1.7	4.9 ± 1.4	1.000
1,2-1,2-16:0/22:6DG	15.2 ± 3.5	10.5 ± 3.1	0.997
1,2-18:0/18:1DG	11.5 ± 2.6	8.9 ± 1.7	0.999
1,2-18:0/18:2DG	21.9 ± 3.2	16.8 ± 3.2	0.997
1,2-18:0/20:4DG	56.5 ± 7.0	41.1 ± 9.3	0.421
1,2-18:0/22:6DG	18.8 ± 4.8	13.1 ± 4.4	0.997
1,2-18:2/18:1DG	58.0 ± 10.5	38.9 ± 5.5	0.147
1,2-di16:0DGa	13.5 ± 2.1	12.0 ± 1.4	0.999
1,2-di18:0DGa	5.2 ± 0.6	5.0 ± 1.3	1.000
1,2-di18:1DGa	31.4 ± 8.1	22.8 ± 3.9	0.958
1,2-di18:2DGa	42.5 ± 8.5	27.7 ± 6.0	0.456
Total DAGs	353 ± 67	261 ± 47	0.313

40

41 DAG content, determined by LC/MS, in LV homogenates from 6-month old male and female

42 offspring of control (Con) and obese (Ob) dams. Con and Ob groups compared by Student's t-test

43 with Holm-Sidak multiplicity correction. [a]Log transformed prior to statistical analysis. *, P<0.05.

44 Mean ± SEM.

45

46 **Suppl. Table 6. Effect of maternal obesity on adult offspring myocardial ceramide content.**

47

pmol/mg protein	Con	Ob	P value (t-test)
Males	n=6	n=5	
16:0Cer	7.8 ± 2.2	3.5 ± 1.0	0.852
18:0Cer	5.1 ± 1.4	2.3 ± 0.6	0.852
20:0Cer	13.5 ± 5.3	7.0 ± 1.9	0.390
22:0Cer	16.6 ± 4.6	8.2 ± 1.8	0.181
24:0Cer	5.5 ± 1.3	3.8 ± 0.7	0.852
24:1Cer	8.1 ± 1.9	4.2 ± 1.1	0.777
Total ceramides	56.6 ± 16.4	29.0 ± 6.8	0.182
Females	n=8	n=6	
16:0Cer	12.0 ± 2.7	11.4 ± 2.2	1.000
18:0Cer	9.1 ± 1.8	8.5 ± 1.8	1.000
20:0Cer	14.7 ± 3.1	14.4 ± 2.8	1.000
22:0Cer	19.0 ± 3.3	20.2 ± 5.0	1.000
24:0Cer	8.3 ± 1.8	8.7 ± 1.5	1.000
24:1Cer	10.2 ± 2.2	10.1 ± 2.1	1.000
Total ceramides	73.3 ± 14.5	73.3 ± 14.9	0.999

48

49 Ceramide content, determined by LC/MS, in LV homogenates from 6-month old male and female
50 offspring of control (Con) and obese (Ob) dams. Con and Ob groups compared by Student's t-test with
51 Holm-Sidak multiplicity correction. Mean ± SEM.

52

53 **SUPPLEMENTARY FIGURE LEGENDS**

54 **Suppl. Fig. 1 *Pparg* is a critical node in the transcriptional effects of maternal obesity on the fetal**

55 **heart.**

56 (A, B) Venn diagrams to show numbers and intersections of up- and down-regulated genes in male

57 and female fetuses. (C, D) Cellular location and direct molecular interactions of differentially

58 expressed, metabolism-related genes in E18.5 male and female fetuses of obese dams. (E) Regulator

59 effects network identified from differentially expressed genes in male fetuses of obese dams. RNASeq

60 data annotated and figures generated by Ingenuity Pathway Analysis. Red symbols indicate

61 upregulated genes, green symbols indicate downregulated genes. Orange arrows indicate predicted

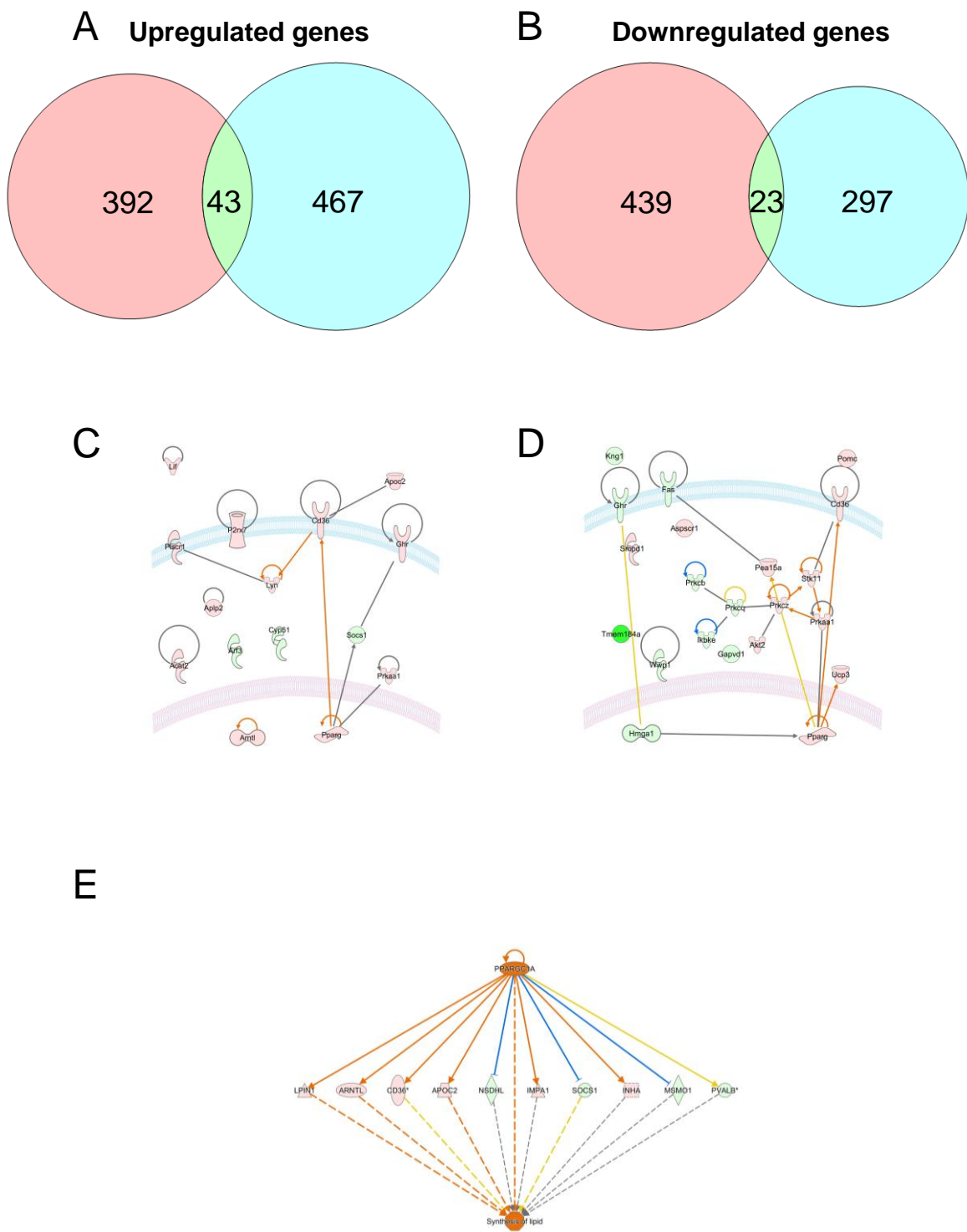62 activation, blue arrows indicate predicted inhibition.

63 **Suppl. Fig. 2 Maternal obesity does not alter left ventricular systolic function or wall thickness in**

64 **adult offspring**

65 (A, B) Ejection fraction, (C,D) fractional shortening, (E, F) wall thickness in diastole and (G, H) wall

66 thickness at systole in male (A, C, E, G) and female (B, D, F, H) offspring of control and obese dams at

67 3, 6, 9 and 24 months after birth. Main effects of maternal obesity and postnatal age, and their

68 interaction, were determined by two-way ANOVA and P values given in figure. Bars are mean ± SEM.

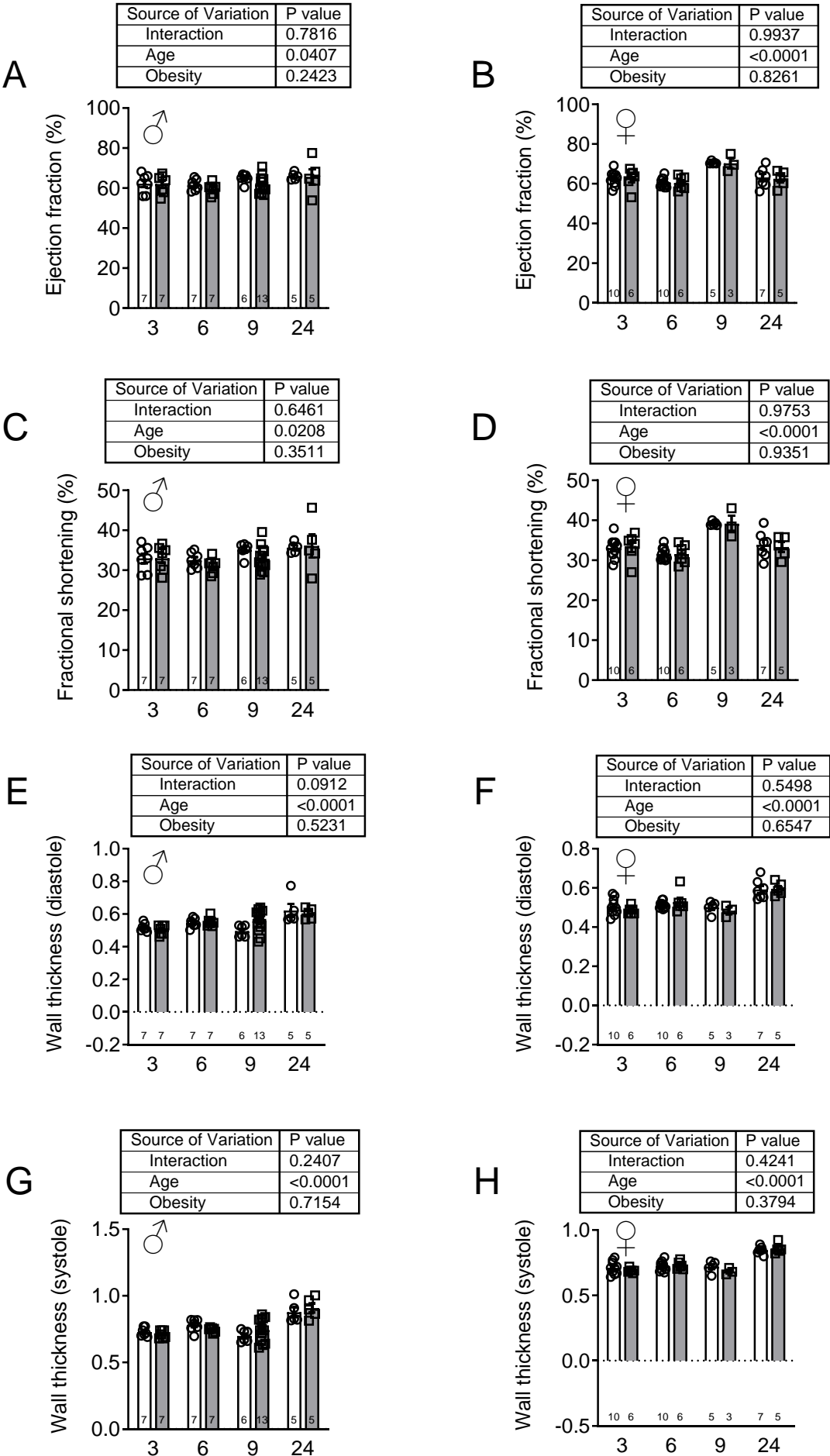69 Symbols represent individual animals. n values given in bars.

70 **Suppl. Fig. 3 Cardiac *in vivo* fatty acid and glucose uptake differ between female and male offspring**

71 **of control dams.**

72 (A) Left ventricular 3H-oleic acid clearance in female (Con n=3) and male (Con n=7) offspring. Con and

73 Ob groups by Student's t-test, Symbols represent individual offspring. (B,C) Left ventricular 8F-

74 fluorodeoxyglucose clearance in female (Con n=10) and male (Con n=8) offspring of control and obese

75 dams (B) Patlak plot, symbols represent mean ± SEM values for all individuals within each group, at

76 each normalized time point. (C) Histogram of mean ± SEM clearance (gradient of Patlak plot) for each

77 experimental group. P values given in figure. Mean ± SEM.

78

7

Suppl. Fig. 1 *Pparg* **is a critical node in the transcriptional effects of maternal obesity on the fetal heart.**

A **Upregulated genes**

B **Downregulated genes**

C

D

E

Suppl. Fig. 2 Maternal obesity does not alter left ventricular systolic function or wall thickness in adult offspring

Source of Variation	P value
Interaction	0.7816
Age	0.0407
Obesity	0.2423

A

Source of Variation	P value
Interaction	0.9937
Age	<0.0001
Obesity	0.8261

B

Source of Variation	P value
Interaction	0.6461
Age	0.0208
Obesity	0.3511

C

Source of Variation	P value
Interaction	0.9753
Age	<0.0001
Obesity	0.9351

D

Source of Variation	P value
Interaction	0.0912
Age	<0.0001
Obesity	0.5231

E

Source of Variation	P value
Interaction	0.5498
Age	<0.0001
Obesity	0.6547

F

Source of Variation	P value
Interaction	0.2407
Age	<0.0001
Obesity	0.7154

G

Source of Variation	P value
Interaction	0.4241
Age	<0.0001
Obesity	0.3794

H

Suppl. Fig. 3 Cardiac *in vivo* fatty acid and glucose uptake differ between female and male offspring of control dams.
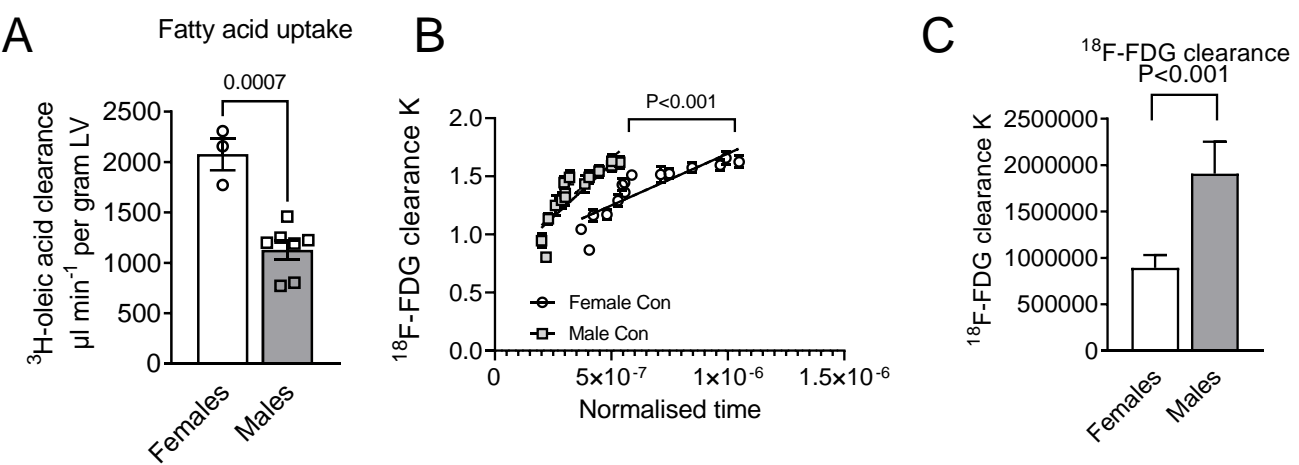
1   **SUPPLEMENTARY METHODS**

2   **Echocardiography**

3   Mice were anaesthetised (2% isoflurane, inhaled), placed in dorsal recumbency on a heated mat

4   maintained at 37°C and hair removed from the thorax using a depilating cream. The heart was imaged

5   in the parasternal short axis, at the level of the papillary muscle, by a trained operator blinded to the

6   treatment group of the animal, using the Vevo 2100 system (VisualSonics). M-mode images of the left

7   ventricle were collected across at least four consecutive cycles and used to measure ventricular wall

8   thicknesses and chamber diameter in systole and diastole. Left ventricular internal volumes at systole

9   and diastole were determined using the leading-edge method then ejection fraction and fractional

10   shortening were calculated as indices of systolic function. Doppler velocimetry was used to determine

11   peak mitral inflow in early (E) and late (A) diastole whilst tissue Doppler was used to determine peak

12   ventricular wall displacement at the level of the mitral annulus, again in early (E') and late (A') diastole.

13   E/A, E'/A' and E/E' ratios were calculated as indices of ventricular diastolic function. Mice were

14   recovered from anaesthesia following echocardiography and returned to their home cage.

15   **RNA sequencing**

16   Sequencing libraries with unique barcodes were constructed from 100 ng of total RNA using the KAPA

17   Stranded mRNA-Seq kit (Kapa Biosystems, Wilmington, MA) according to the manufacturer's protocol.

18   Individual cDNA libraries were quantified by qPCR. Pooled libraries were used to generate clusters by

19   cBot with version 3 reagents (Illumina, San Diego, CA). Multiplex paired-end (2 x 100 base) sequencing

20   was performed on the HiSeq 2500 Sequencing System with version 3 SBS chemistry (Illumina).

21   Sequencing reads were demultiplexed using the CASAVA pipeline (Illumina) and then aligned to the

22   *Mus musculus* reference genome (mm10) using STAR version 2.5.3a in Partek Flow (Partek, St. Louis,

23   MO). Aligned reads were quantified using the Expectation/Maximization algorithm in Partek Flow with

24   RefSeq transcripts from NCBI annotation release 84. Transcripts with zero read counts across all

25   samples were removed prior to performing normalization of read counts using the Trimmed Mean of

1

26 M-values method [46]. Afterwards, transcripts with at least 5 read counts across all samples were

27 included for comparing expression in Ob vs. Con, separately in male and female fetuses. The Gene-

28 Specific Analysis in Partek Flow was used for differential expression analysis, in which the best

29 statistical model was identified for each transcript based on the normalized read counts of that

30 transcript and the best model was used to produce the fold change, P values and P values adjusted by

31 the method of Benjamini and Hochberg [47].

32 **Ingenuity Pathway Analysis**

33 Differentially expressed mRNAs were functionally annotated *in silico* using Ingenuity Pathway Analysis

34 (IPA) software (Qiagen). Downstream biological processes predicted to be affected by maternal

35 obesity were identified using an unbiased approach based on significant enrichment with differentially

36 expressed genes. The direction of expression change of mRNAs within each gene set was used to

37 predict overall activation status of the pathway or function, by calculating a z-score, such that negative

38 z-scores represented inhibited pathways and positive z-scores represented activated pathways.

39 Functions were filtered for further investigation based on a threshold of z-score > $|1.7|$ and ranked

40 by significance level (P-value). Downstream functions commonly affected by maternal obesity in both

41 female and male fetuses were identified using unsupervised comparative analysis in IPA.

42 Unsupervised upstream regulator analysis within IPA was also used to identify key molecules (e.g.

43 transcription factors) predicted to cause the observed transcriptional effects of multiple differentially

44 expressed genes.

45 **Targeted lipidomic analyses**

46 For fatty acid quantification, frozen ventricular tissue was homogenised in hepes-tris buffered saline

47 solution then lipids were extracted using a liquid-liquid extraction method, as described (Chassen et

48 al, 2018). Briefly, an aliquot of ventricle homogenate was deproteinised by addition of methanol, with

49 vortexing, then centrifuged (500g, 15 min, at room temperature). The supernatant solution was

50 transferred to a glass vial, water and dichloromethane were added to extract lipids, vortexed and

2

51   centrifuged. The polar lipid lower layer was separated and dichloromethane extraction was repeated

52   with the upper aqueous layer. Combined lipid layers were dried under N_2, resuspended in ethanol

53   then spiked with an internal FA standard solution. Lipids were saponified with 1M NaOH at 90°C for

54   1hr, neutralised, extracted into isooctane and derivatized using pentafluorobenzyl bromide and

55   diisopropylethalamine in acetonitrile. The final fatty acid extract was resuspended in isooctane for GC-

56   MS analysis. Samples were separated on a HP-5MS capillary column (30m, 0.25mm, 0.10mm film

57   thickness, Agilent), subjected to mass spectrometry then identified and quantified based on *m/z* ratios

58   and peak heights, respectively [48].

59   For quantification of ceramides and diacylglycerol (DAG) species, heart samples homogenized in 900

60   µL water and an aliquot (20 µL) taken for protein concentration. Methanol (900 µL) was added to the

61   homogenized sample (750 µL). After the addition of 15:0/18:1(d_7)-DAG (80 pmol) and 12:0-ceramide

62   (80 pmol) as internal standards, lipid extraction was performed by the addition of methyl-*tert*-butyl

63   ether (3 mL) according to Matyash et al [49]. The organic phase was dried under a stream of nitrogen

64   gas and resuspended in 400 µL of a mixture of 70/30 (v/v) hexane:methylene chloride. Samples were

65   injected into an HPLC system connected to a triple quadrupole mass spectrometer (Sciex 2000 QTRAP,

66   Framingham, MA) and normal phase chromatography with a HILIC column (100x2.1 mm, Kinetex HILIC

67   2.6 µm, Phenomenex) was used to separate lipids by class [50]. Mass spectrometric analysis was

68   performed in the positive ion mode using multiple-reaction monitoring (MRM) of DAG and ceramide

69   molecular species and the internal standards. Quantitation was performed using stable isotope

70   dilution with a standard curve for DAGs and ceramides and results were normalized to protein

71   content. All lipid measurements were expressed relative to tissue protein content, determined by

72   bicinchoninic acid assay.

73